Thatchbed Island Erosion and Mitigation Options Study

An investigation into erosion and potential interventions around Thatchbed Island in Essex, CT

Marc de Vos, Yaprak Onat, Kay Howard-Strobel, Alejandro Cifuentes-Lorenzen, and James O'Donnell

Connecticut Institute for Resilience and Climate Adaptation

and

Department of Marine Sciences

University of Connecticut

November 2025

CIRCA Project Team:

- Prof. James O'Donnell – Executive Director of CIRCA and Professor at the Department of Marine Sciences at UConn
- Dr. Yaprak Onat – Associate Director of Research and Project Principal Investigator
- Dr. Marc De Vos – Research Associate
- Dr. Alejandro Cifuentes-Lorenzen – Research Associate Scientist
- Kay Howard-Strobel – Research Associate
- Carson Hill – Oceanographic Research Assistant
- Nathan Robinson – Research Assistant

Citation for the report: De Vos, M., Onat, Y., Howard-Strobel, K., Cifuentes-Lorenzen, A., and O'Donnell, J. (2025). "Thatchbed Island Erosion and Mitigation Options Study," University of Connecticut, Connecticut Institute for Resilience and Climate Adaptation, Groton, CT.

This project has been funded wholly or in part by the United States Environmental Protection Agency under assistance agreements LI-00A00579-0 to the Connecticut Department of Energy and Environmental Protection. The contents of this document do not necessarily reflect the views and policies of the Environmental Protection Agency, nor does the EPA endorse trade names or recommend the use of commercial products mentioned in this document.

More information on CIRCA can be found at: www.circa.uconn.edu

Contents

List of Acronyms

D3D – Delft3D FLOW

DEM – Digital Elevation Model

DSAS – Digital Shoreline Analysis System

EPR – End Point Rate

FVCOM – Finite Volume Community Ocean Model

LRR – Linear Regression Rate

MHW – Mean High Water

MLW – Mean Low Water

MSF – Morphological Scale Factors

MSL – Mean Sea Level

NAVD88 – North American Vertical Datum of 1988

NOAA – National Oceanic and Atmospheric Administration

NSM – Net Shoreline Movement

SCE – Shoreline Change Envelope

TWL – Total Water Level

USGS – United States Geological Survey

List of Figures

Executive Summary

Thatchbed Island is a tidal marsh feature in the lower Connecticut River at Essex that has experienced sustained erosion over recent decades, with the most rapid losses concentrated at the marsh's southeastern spit. This report includes the results of the investigation into erosion around Thatchbed Island in Essex, Connecticut. The investigation consisted of historical shoreline analysis, observational and modeling components, site visits and interviews.

Using the USGS Digital Shoreline Analysis System (DSAS), we analyzed 238 transects spanning 1991–2023 and found persistent, statistically significant regression-based retreat averaging 1.77 ft/yr, with the largest land loss and positional mobility along the eastern spit. This spatial pattern aligns with the island's platform morphology and measured hydrodynamics in adjacent shallows.

The observational component involved two field campaigns (fall 2024 and spring 2025) during which measurements of sediment characteristics and hydrodynamics were collected at various times and locations near Thatchbed Island. The field program deployed ADCPs in the channel and nearshore to estimate currents, water levels, and bed shear, and collected 20 sediment samples to define local grain-size distributions used to initialize model sediment classes. The purpose of this component was to assemble the data and information required to build and calibrate a hydrodynamic and morphological numerical model of the domain.

The modelling component involved developing a bespoke numerical model to simulate the hydro-morphological dynamics of the area around Thatchbed Island. Modelling also enabled testing of community-proposed erosion control interventions (generically referred to as "geo-textile tubes" or "geotubes"), to assess effectiveness and potential downstream impacts. This representation is structure-agnostic. In other words, the modeled performance reflects a low-crested barrier of the tested footprint and crest control, whether built with geotextile tubes or stone sills of comparable geometry.

Following calibration of the model involving around 100 simulations, nine core simulation experiments that represent realistic forcing (three periods covering differing river discharge and tidal range) and three structure scenarios: baseline (no structure) and two containment alignments that represent the community's concept of a nearshore containment sill with backfill between the sill and island (a longer "Configuration 1" and a shorter "Configuration 2").

Model Results indicate that Envirotube deployments and backfill substantially reduced erosion in the vicinity of the southeastern tail of Thatchbed Island, where the shoreline is most vulnerable to flow acceleration. Introducing a barrier with backfill deflects that jet offshore, producing a sheltered wake and reducing bed lowering landward of the alignment. The magnitude and spatial extent of protection varied across flow regimes, yielding more pronounced benefits under more erosive regimes and muted impacts under weaker forcing regimes. The larger of two deployment configurations tested provided greater shoreline protection than the smaller deployment, though both designs produced consistent sheltering directly landward of the tubes. During weaker forcing, the differences between configurations were minimal, with both yielding comparable reductions in local bed lowering. Across all simulations, areas of erosion and deposition were localized, confined mainly to the regions near the deployments. Model results suggest that significant remote or far-field morphological impacts are unlikely.

To complement modeling with operational experience, we conducted interviews and site visits in West Galveston Bay, Texas, which has more than two decades of experience with geotextile tube implementation. Interviews and site observations indicate that geotextile tube systems can achieve near-term goals at lower initial cost when access limits stone delivery, but they carry higher operational and maintenance risk in busy waterways and are vulnerable to damage, therefore they are abandoned for further use in that area.

Given the energy regime, vessel traffic, and navigation constraints of the Connecticut River near the Essex reach, recommendations can include a phased, pilot-first strategy that: (1) proves constructability and verifies performance at the southeast tail; (2) sets crest and gaps in datum and surveys them; (3) specifies sand fill and scour protection where geotextile is used, with robust end treatments to resist flanking; (4) pairs the installation with an signage/marking plan and seasonal inspections; and (5) defines quantitative success metrics (lee-platform elevation gain, reduction in modeled/measured bed lowering, vegetation establishment). Final selection among alternatives should weigh material-specific durability, maintenance burden, and navigation safety in addition to the hydrodynamic benefits demonstrated here.

1. Introduction

Thatchbed Island is a tidal marsh island in the lower Connecticut River at Essex, immediately south of the Essex Yacht Club and within the Connecticut River estuary complex. The marsh is part of a region designated as internationally important under the Ramsar Convention. Most of Thatchbed Island is owned by the Essex Land Conservation Trust with some state ownership, which places the site within a conservation and public trust context for management actions (Figure 1).

Historic materials from the town and local land trust describe a larger marsh footprint through the twentieth century that has contracted markedly in recent decades. A 2024 Essex Land Trust note reports that the feature once extended to nearly 30 acres and is now less than seven acres, with visible vegetation loss from year to year (Sealey, 2024). The harbor has long contained rock features along the eastern side of the former island alignment. Town records indicate that these stone piers predate 1950 and have been identified as a hazard to navigation for more than 25 years, which is relevant to shoreline processes and to design constraints for any restoration works.

Essex formed an Ad Hoc Thatchbed Island Committee to understand the causes of erosion and to develop a plan that restores lost marsh using environmentally conservative methods. The committee's work program emphasizes beneficial use of clean dredged material consistent with guidance from the Environmental Protection Agency and the United States Army Corps of Engineers. The town has engaged residents to collect local ecological knowledge for the Essex Harbor setting. Since 2024, the committee has advanced a concept that places large geosynthetic tubes as containment for dredged material and then seeds the backfilled area with marsh grasses. The committee is in the process of permit submission to the Connecticut Department of Energy and Environmental Protection (CT DEEP) and subsequent procurement steps in 2025 to solicit qualified contractors for tidal wetland restoration at Thatchbed Island.

Project Goal and Scope

CIRCA is contracted by CT DEEP to analyze the causes of the Thatchbed Island erosion that has occurred over the last decade, assess the potential utility of the Geotube/Envirotube technologies (as proposed by local stakeholders) in preventing further erosion, and develop design concepts that would allow the Thatchbed Island to serve a model for shoreline stabilization and habitat restoration through reuse of

dredged materials from nearby harbors. This project provides the technical basis for near-term decisions on stabilization and restoration of Thatchbed Island. The scope includes

i. Erosion Analysis: Conduct a thorough evaluation to identify and understand the root causes and factors contributing to erosion in the specified area.
ii. Envirotube Efficacy Evaluation: Review and summarize the literature and perform site visits to summarize the expected performance and overall effectiveness of geotubes/Envirotubes in addressing and mitigating the identified erosion issues.
iii. Alternative Solutions Exploration: Investigate and recommend potential alternatives to geotubes/Envirotubes that can offer comparable effectiveness in erosion control and prevention. This will involve researching existing methods and innovative solutions and assessing their feasibility in the context of the project area.

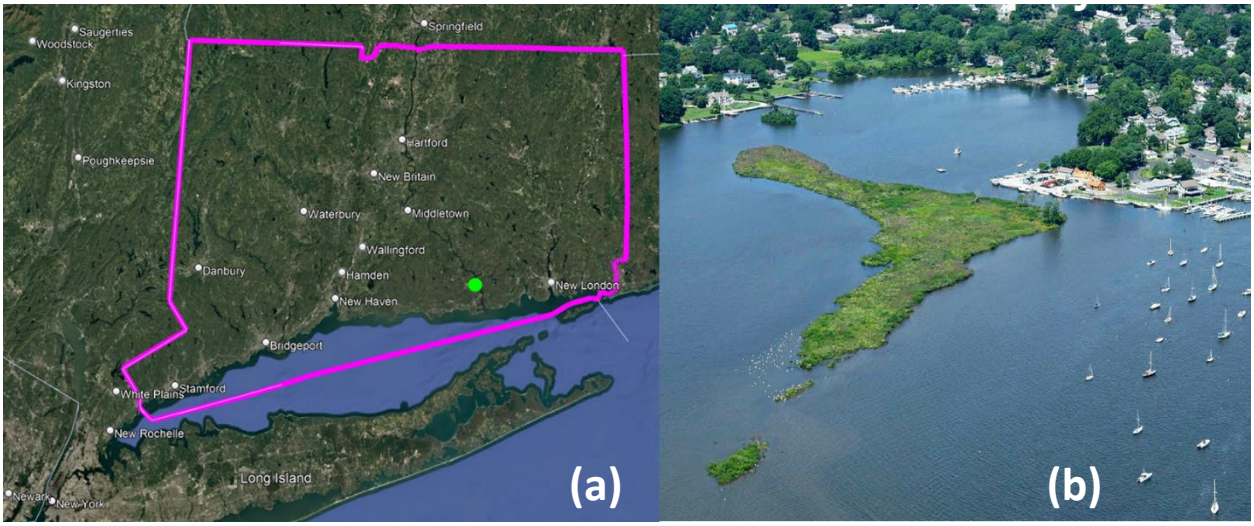

Figure 1. Context map (a) showing the Connecticut state boundary (magenta) and study site (green dot). Panel (b) shows an oblique aerial view of Thatchbed Island in the Connecticut River at Essex. The southeastern tail of the island (and site of major erosion) is visible in the bottom left corner of panel (a).

The project aims to determine the causes, patterns, and rates of erosion at Thatchbed Island and to translate those findings into practical restoration options. We first quantify shoreline change and diagnose the processes driving loss to establish a defensible baseline for design. Building on that analysis, we evaluate the expected performance, constructability, durability, and ecological implications of geosynthetic tube containment for beneficial use of nearby dredged material, as proposed by local stakeholders. In parallel, we review and compare alternative protection strategies of comparable effectiveness, including stone sills and other low crested structures, to identify where each approach is

feasible given exposure, navigation, and sediment conditions. Using these evaluations, we develop concept designs that couple containment and fill volumes with crest and toe targets, gap treatments, and access logistics suitable for permit review. We conclude with a monitoring and adaptive management framework that repeats the shoreline analysis, surveys control elevations, tracks vegetation establishment, and documents maintenance needs so the town can implement and adjust a cost effective, permittable demonstration of dredged material reuse at Thatchbed Island.

2. Data and Methods

2.1 Digital Shoreline Analysis

We evaluated multi-decadal shoreline change at Thatchbed Island using the U.S. Geological Survey Digital Shoreline Analysis System version 5.1, operating within Esri ArcGIS Desktop. DSAS computes rates and distances of shoreline change from a time series of vector shorelines by casting orthogonal transects from a user-defined baseline and then calculating statistics along each transect. The software provides standardized outputs for the shoreline change envelope (SCE), net shoreline movement (NSM), end-point rate (EPR), linear regression rate (LRR), and weighted linear regression, with associated confidence information.

Input shoreline dates spanned 1991 through 2023 (Figure 2). We used a five-meter (16.4 ft) transect spacing, a ten-meter (32.8ft) smoothing distance, a 90% confidence interval, and a default shoreline position uncertainty of 30 meters (98.43 ft). The coordinate system was WGS 1984 UTM Zone 18N. No proxy datum bias was applied. The reported metrics include:

The Shoreline Change Envelope (SCE) is the distance to the greatest separation among all shoreline positions intersected by a transect. It is always positive. Net Shoreline Movement (NSM) is the distance between the oldest and most recent shorelines along a transect. Dividing NSM by elapsed time yields the End Point Rate. End Point Rate (EPR) is the NSM distance divided by the time between the oldest and most recent shoreline. Linear Regression Rate (LRR) is the slope of a least squares line fit to all shoreline dates along a transect. It uses all positions and reports supporting statistics, including standard error and confidence interval. Weighted Linear Regression Rate applies date-specific weights but is reported with the same supporting statistics. DSAS also reports a reduced “n” value, which estimates the number of

independent transects and is used to compute the uncertainty of the regional average rate. This guards against overstating certainty when adjacent transects sample the same processes.

The analysis included 238 transects. All distances are given in meters, and all rates are meters per year.

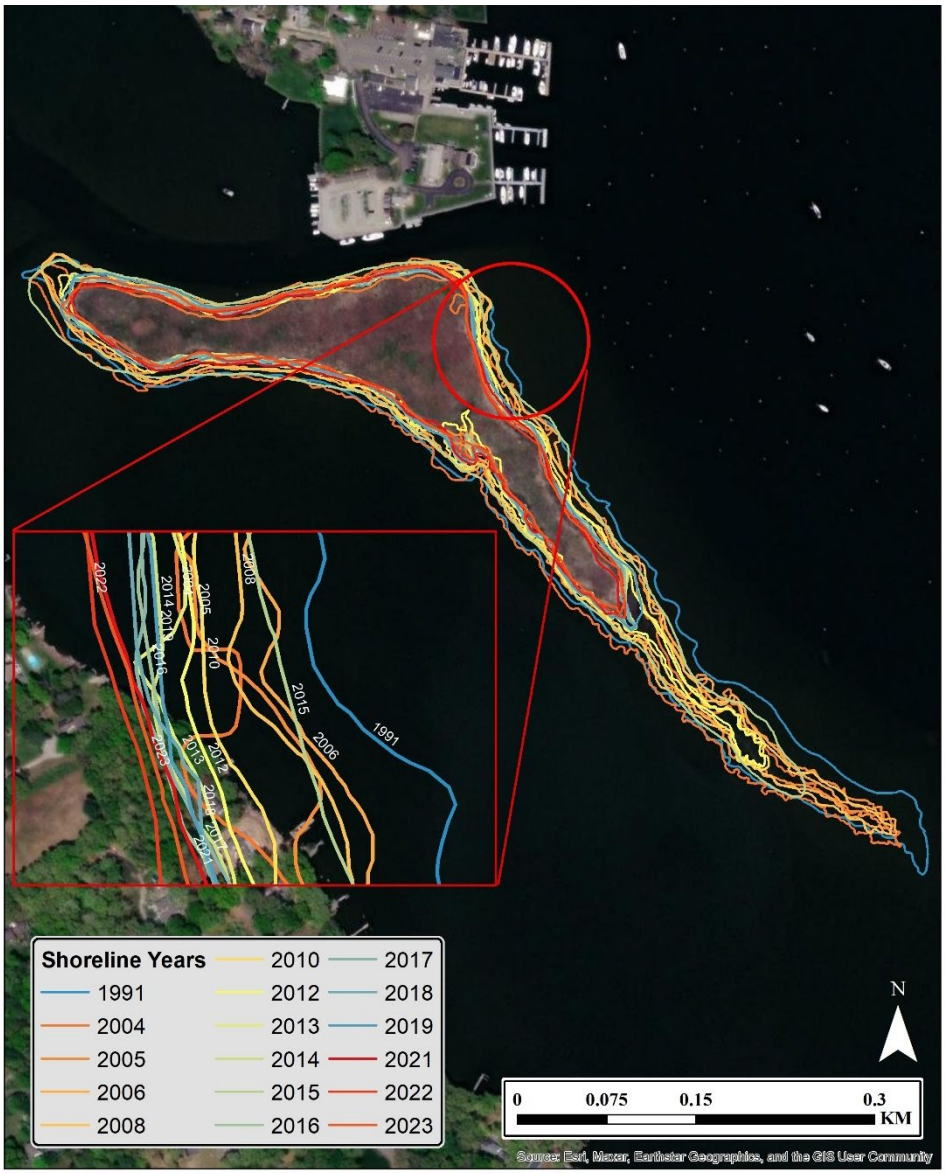

Figure 2. Time series map with inset showing all extracted shoreline positions from 1991 to 2023 and a detail of the western shore.

Shoreline Change Envelope: Average SCE was 22.96 with a minimum of 10.29 at transect 88 and a maximum of 256.51 at transect 194. These values quantify the total excursion of the shoreline footprint across the record and delineate the highest mobility along the eastern spit (Figure 3).

Net Shoreline Movement: Average NSM was −15.94. Erosional transects comprised 196 of 238, which is 82.35 percent. Maximum erosion was −251.53 at transect 194. Maximum accretion was 4.55 at transect 71. These values indicate net land loss across most of the perimeter with localized gain on the interior margin (Figure 4).

End Point Rate: Average EPR was −0.50. At the chosen confidence level, the average EPR uncertainty using reduced n was 1.33, indicating that the regionally averaged endpoint signal is not statistically distinct from zero when considered alone. Only 1.68 percent of transects showed statistically significant erosion by EPR. Maximum erosion rate was −7.86 at transect 194, and maximum accretion rate was 0.14 at transect 71 (Figure 5).

Linear Regression Rate and Weighted Linear Regression Rate: Average LRR and WLR were both −0.54 with reduced n equal to 37 and an average rate uncertainty of ±0.04 for the region. Erosional transects were 87.39% of the total and 73.11% of transects exhibited statistically significant erosion. Maximum erosion rate by regression was −11.07 at transect 194. The maximum accretion rate was 0.10 at transect 93. The weighted regression reproduced the same regional averages for this dataset.

The DSAS analysis shows that

1. The dominant pattern is persistent erosion around most of the island with the strongest losses concentrated near the eastern spit where both NSM and all rate metrics reach their most negative values at transect 194. The SCE maximum at the same location confirms large positional excursions that align with the narrow spit morphology.
2. EPR provides a consistent sign and magnitude with NSM, but its regional average is not well resolved in a statistical sense due to the very small, reduced n. This reflects the spatial correlation of adjacent transects and the sensitivity of a two-date metric to the choice of start and end years. For design and planning, we rely primarily on regression-based rates, which use the full time series and have well-constrained regional uncertainty.
3. Regression results indicate a coherent erosional signal through the 1991 to 2023 period. The high fraction of statistically significant negative rates suggests that the observed losses are not an artifact of individual outlier shorelines. The weighted and unweighted regressions converged, which implies that recent years have not departed strongly from the long-term trend at the scale of this analysis.

4. All DSAS computations were made with a 90% confidence interval. The default shoreline uncertainty of 30 meters was applied when per-date uncertainties were unavailable. These settings propagate into the EPR uncertainties and the regression confidence intervals reported by DSAS.

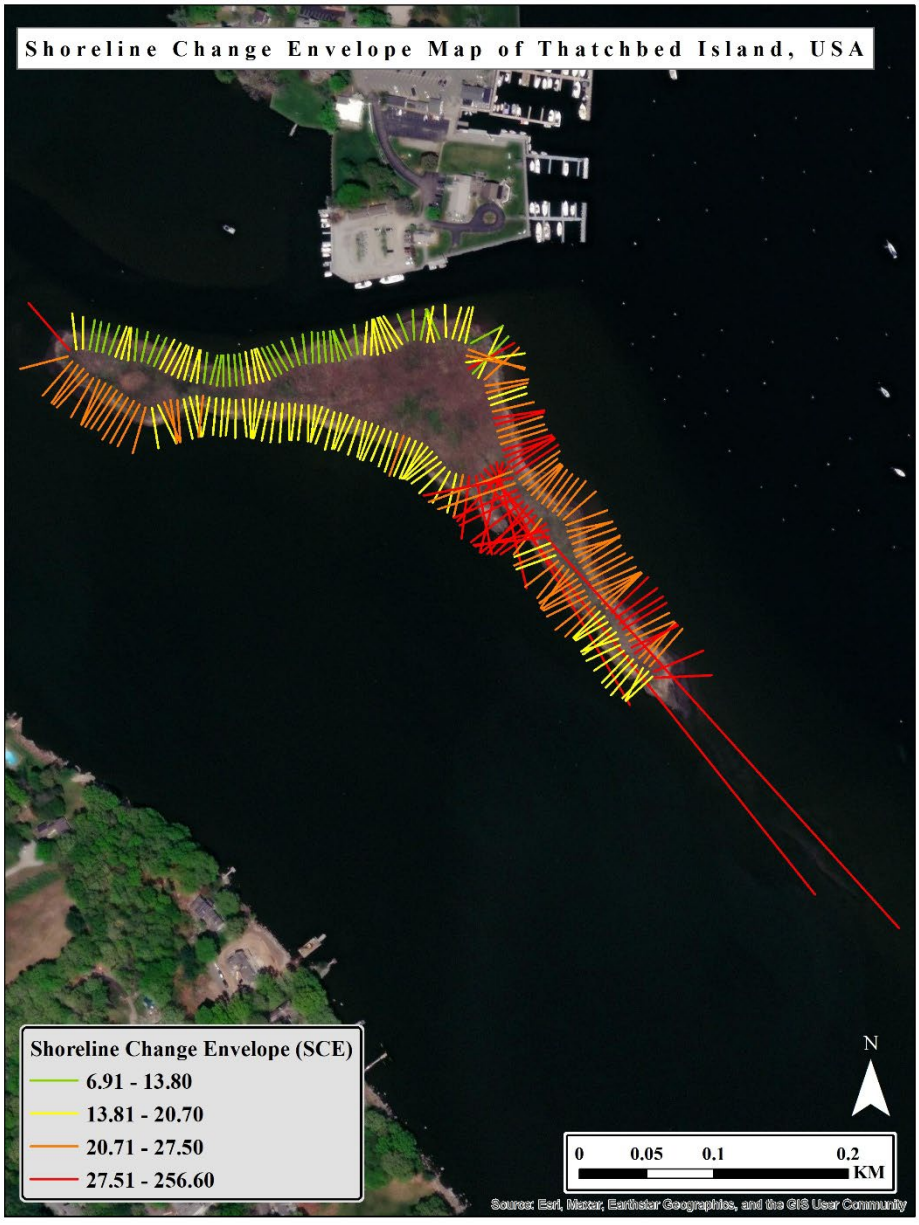

Figure 3. Shoreline change envelope map

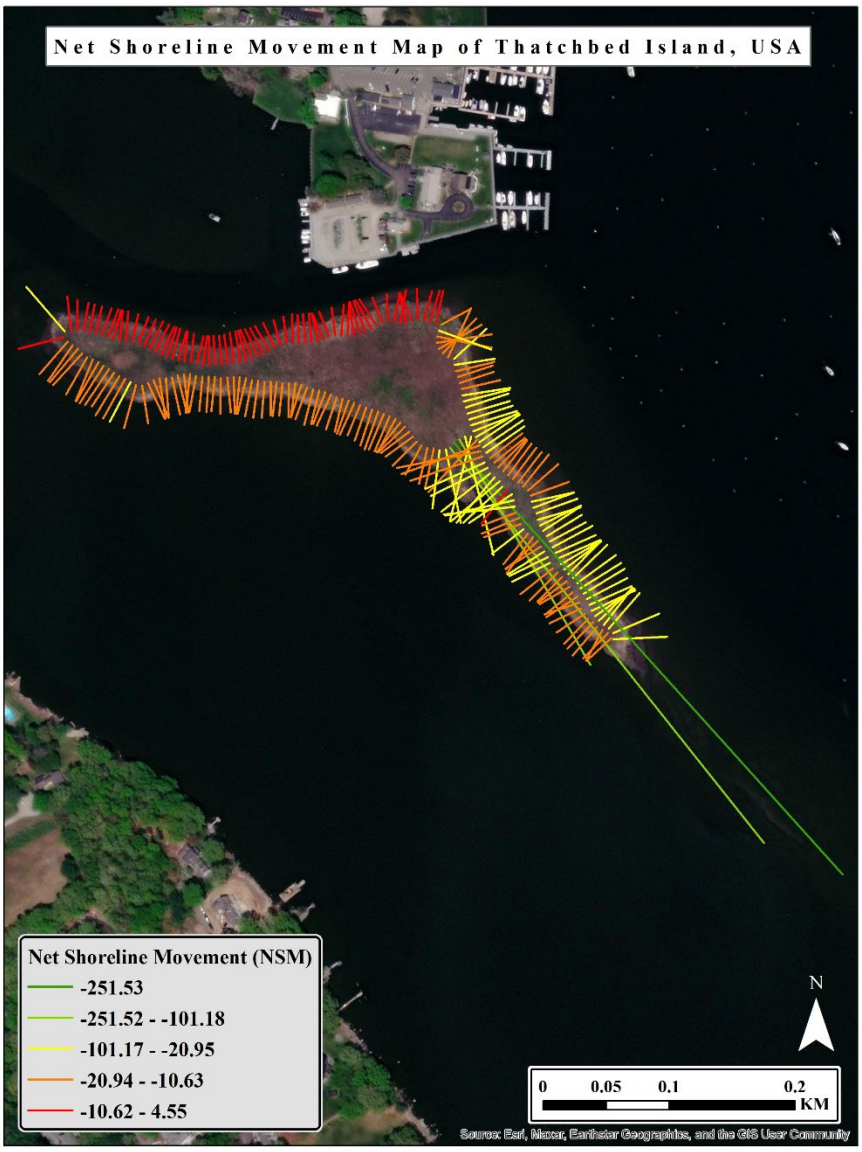

Figure 4. Net shoreline movement map showing net gain or loss along each transect

The DSAS assessment documents sustained erosion of Thatchbed Island from 1991 to 2023, with the greatest mobility and land loss along the eastern spit. Regional averages based on regression methods show a rate of approximately -0.54 meters (-1.77 ft) per year with well-quantified uncertainty. The SCE and NSM fields identify the highest-hazard reaches and provide spatial targets for stabilization concepts and continued monitoring design. The parameter set and outputs documented above establish the baseline against which any future intervention should be evaluated using the same transect geometry and statistical settings for comparability.

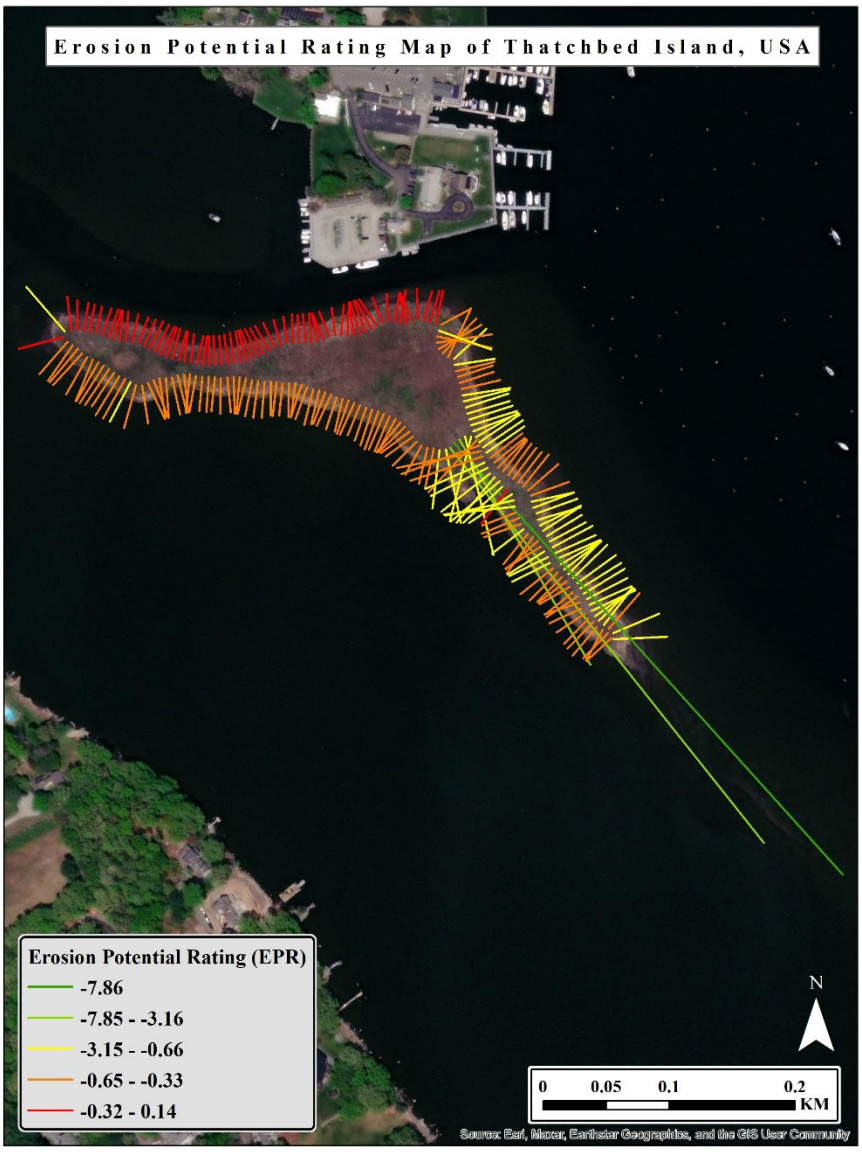

Figure 5. End point rate map derived from oldest and most recent shorelines.

2.2 Observations

Two field campaigns were conducted to collect a range of measurements and data in situ for use in model development and calibration. For comprehensive detail on the field campaigns and associated instrumentation and data, the reader is referred to the accompanying report "Thatchbed Island Field Data Collection & Sediment Grain Size Analysis Summary Report Winter/Spring 2024-2025".

While exact instrument deployment and recovery dates vary slightly, usable data coverage from the campaigns spans two periods during fall and spring, respectively, from 2024-11-08 until 2024-11-26 and 2025-04-02 until 2025-05-06.

Three sets of Nortek Aquadopp up-and-downward looking Acoustic Doppler Current Profilers (ADCPs) were deployed in the river channel and in the shallows near Thatchbed Island, with the aim of collecting measurements to enable the near-bottom turbulence structure, bed shear stresses, water levels, and current velocities to be derived. Figure 6 shows deployment locations for the ADCP instruments. Figure 7 shows a time series summary of the bed shear stresses and velocities, among the most important quantities for sediment transport, computed using observed data from sites tb_1 (upstream of the Island, in the channel) and tb_2 (in the shallows immediately east of Thatchbed Island).

Further, a Ponar grab device was used to collect 20 sediment samples from the area around Thatchbed Island. From these samples, characteristic sediment types and grain sizes were assessed. Figure 8 shows a map of the sediment sample collection locations and the relative proportions of gravel, sand, and mud in each sample. This spatial information was used to inform initial sediment distributions in the sediment model, and grain sizes were assigned to corresponding sediment classes in the model.

Figure 6. Aerial view of the study domain. The green boundary shows the D3D numerical sediment model, whilst markers TB1-3 show the deployment positions of the Nortek Aquadopp instruments deployed during the field campaign.

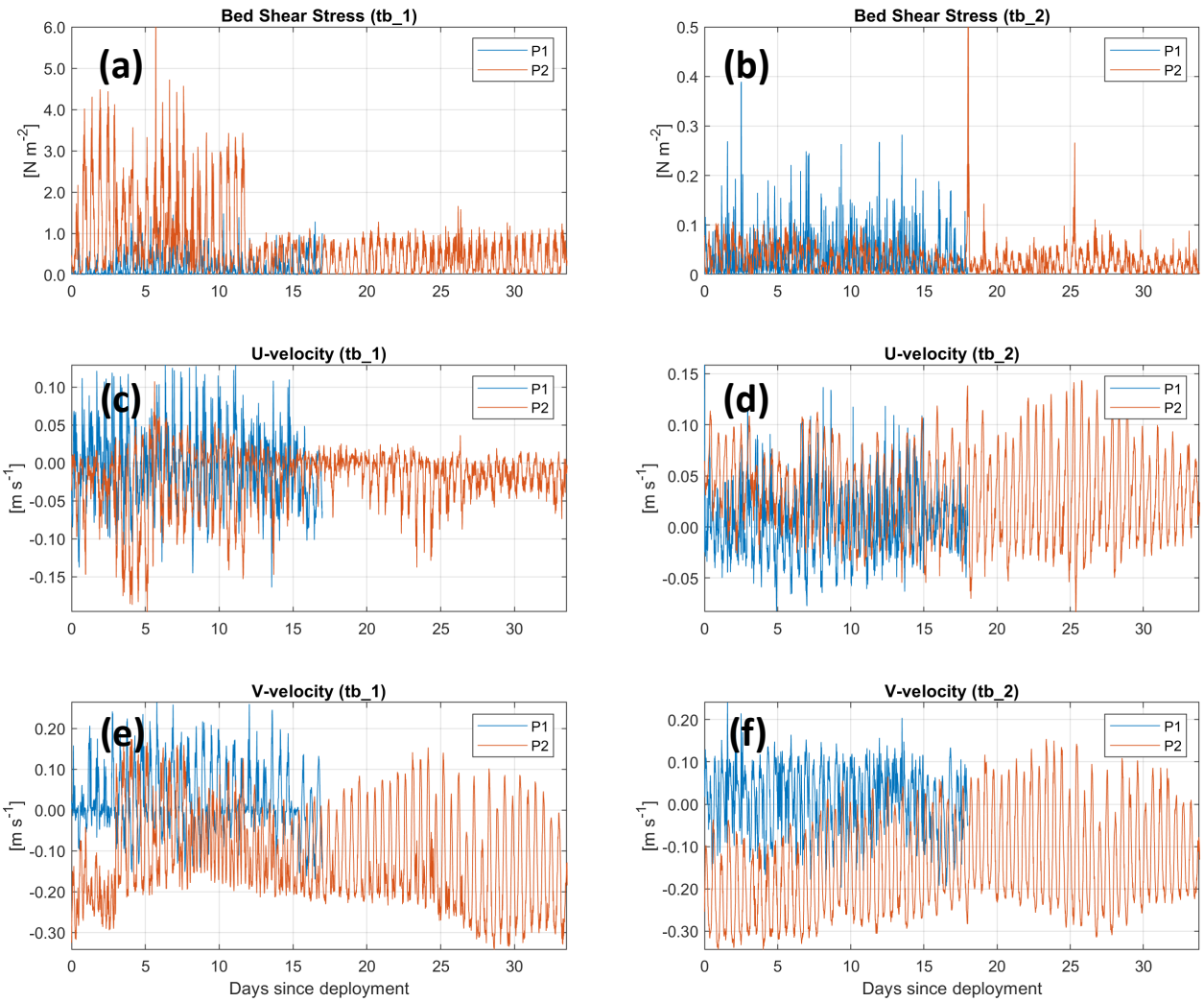

Figure 7. Time series summary of observational data collected near Thatchbed Island. Colors represent different time periods: P1 is the fall period 2024-11-08 until 2024-11-26 and P2 is the spring period 2025-04-02 until 2025-05-06. Panels (a-b) show bed shear stresses, (c-d) show zonal velocity components (roughly cross-channel) and panels (e-f) show meridional velocity components (roughly along-channel).

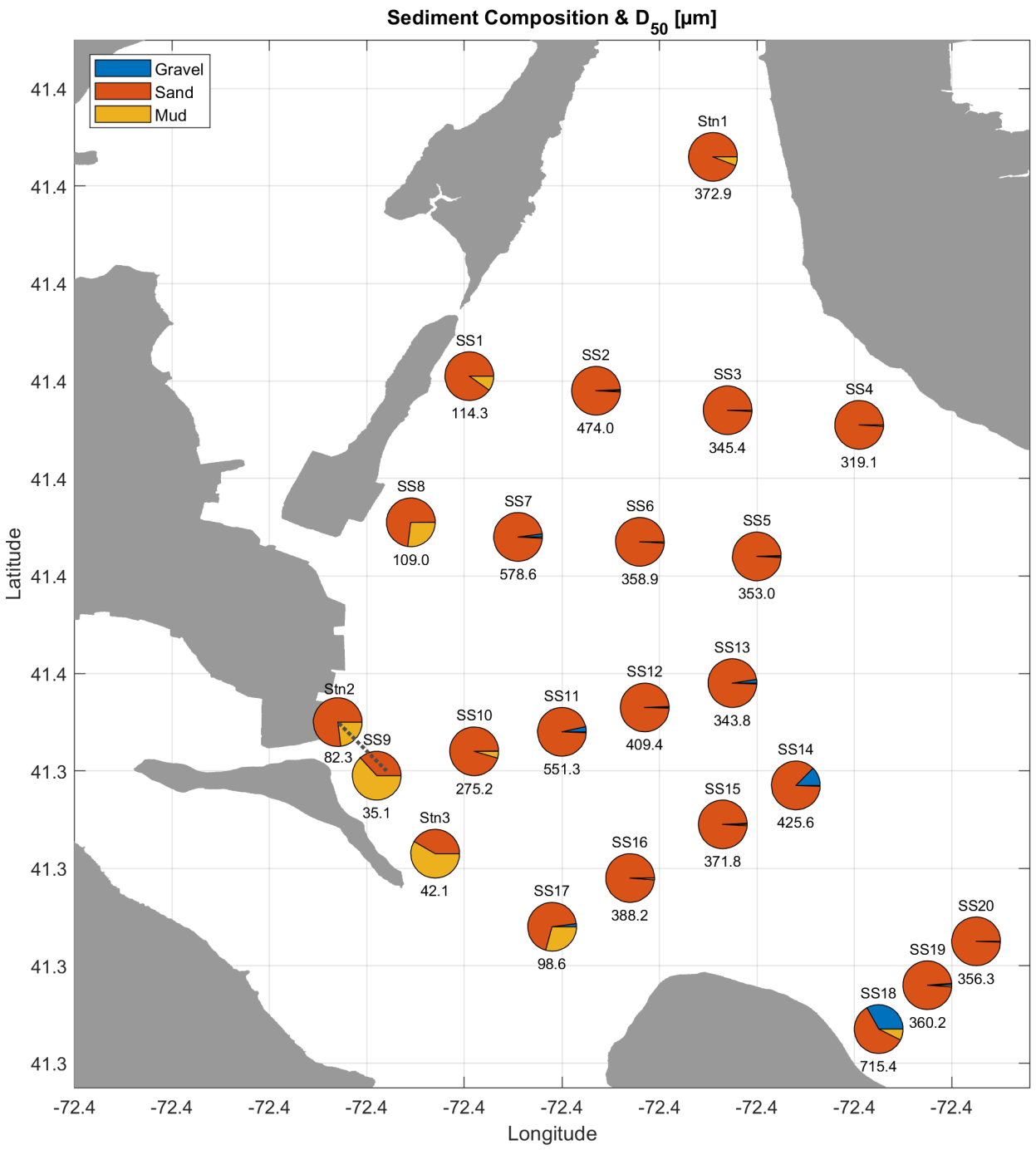

Figure 8. Pie charts showing sediment-type proportions and median diameters at each of the sediment collection locations.

2.3 Site Visits and Interviews

We sought operational experience with geotextile tube projects and nearshore protection systems that have been in service for many years. The interviews are conducted with Texas Parks and Wildlife Coastal Fisheries, the Galveston Bay Estuary Program at the Texas Commission on Environmental Quality, the Coastal Erosion Planning and Response Act Program of the Texas General Land Office, and private companies and engineers who worked with USACE on geotextile systems. We selected Galveston Bay because it offers two decades of documented geotube use across shallow, fetch-limited marsh edges with active small craft traffic, which aligns with the conditions that drive erosion at Thatchbed Island. The setting is not identical, as Galveston Bay is not river-dominated and experiences less ice, but the operational lessons on crest selection, fill quality, toe and end treatments, navigation hazards, and maintenance burden can be transferable to Essex. The interviews focused on design choices, construction and maintenance practices, performance under wave and vessel traffic conditions, ecological response, navigation and safety, permitting, and cost. Site visits and image reviews were used to align observations with the interview content. We gain the following insights:

Design and Construction:

- Tubes function best in quiet waters with moderate fetch and limited vessel traffic.
- Crest elevation is critical. Older installations often had crests near two feet NAVD and were frequently overtopped. Recent projects target about three to four feet NAVD to account for water level variability and sea level rise.
- Sand is the preferred fill material. Silty or clay-rich fill leads to flattened tube geometry and poor crest freeboard.
- Fabric choice involves a trade-off. Woven products are stronger but can allow sand to pass through. Non-woven products are tighter but weaker in tension.
- Scour pads and apron treatments are common at the toe. Passes and gaps require special detailing to avoid flanking.
- Construction is typically scheduled in season when boat traffic and wind are lower than usual. Local sand sources from maintenance dredging or nearshore borrow improve logistics.

Operation and Maintenance:

- Routine maintenance is required. Common tasks include patching punctures, resealing fill ports, replacing short reaches, and re-leveling settled sections.
- Ultraviolet exposure and vandalism degrade the fabric. Shrouds slow the damage but complicate the sealing of the fill port.
- Vessel wakes, anchoring, prop cuts, and fishing activity cause frequent damage in high-use areas.
- Some legacy sites have transitioned to rock sills or segmented breakwaters after repeated failures or the end of service life.

Performance and service life:

- Many sites delivered measurable wave attenuation, accretion in the lee, and improved marsh conditions during the first decade after construction.
- Reported service life varies by exposure and maintenance. Typical design life mentioned by practitioners is 5 to 10 years in energy settings. Some West Galveston Bay sites operated for 15 to 20 years before reinforcement or replacement.
- Monitoring noted modest subsidence on the order of several inches and localized scour at inlets and passes.
- Submerged low crests create navigation hazards. Clear marking and signage are essential.

Environmental and permitting context:

- Site selection has been guided by historical marsh extent, exposure to fetch, and sediment type. Sandy settings are favored. Muddy settings often require rock or clay berms rather than tubes.
- Permitting pathways cited a typical processing time on the order of half a year.
- Costs have been lower than rock construction where access for barges is limited, but prices for fabrics and marine work are rising.

Consensus:

- Tubes can be cost-effective where access is limited by heavy stone and where exposure is modest.
- Performance depends on correct crest elevation, appropriate fill, and robust toe and end treatments.
- Continuous maintenance is not optional. Without active repairs, service life shortens rapidly.

- Human interaction is a major risk driver. Boat traffic and fishing activity are frequent sources of damage.
- Many older tube projects are now capped or replaced with rock structures as they age.

Points of uncertainty:

- Expected service life. Estimates ranged from 5 to 10 years at exposed sites to 2 decades in quiet water with steady maintenance.
- Net sediment response. All interviewees observed wave attenuation and periods of accretion behind the tubes, but the longevity of those gains varied by setting and maintenance history.
- Fabric choice. Practitioners differ on the balance between strength and retention when selecting woven versus non-woven fabrics, and on the value of shrouds relative to the added construction complexity.

From 19-21 August 2025, several site visits were conducted in five main zones in the Galveston (Texas) West Bay area (Figure 9, 10,11). The aim of the site visits was to gather in situ information on geotube deployment. Noteworthy characteristics included aesthetic impact, visibility with respect to tidal elevation, durability, interaction with plants and animals, navigational hazards, signage, and observable function in terms of wave attenuation. Some general findings from the site visit were:

- Geotubes appeared durable and robust, notwithstanding feedback from other users that damage caused by human interference can compromise their integrity.
- Tubes were, in many cases, nearly invisible at high tide. Consideration should be given to implications for navigation.
- Numerous bird species appeared to make frequent use of tubes as perches.
- Tubes were deployed on a scour mat.

Implications for Thatchbed Island

- The island's energetic eastern spit and frequent vessel traffic argue for cautious use of tubes and for careful crest selection if tubes are considered.
- A hybrid system that uses stone at the most exposed reaches and deploys tubes only in lower energy segments is consistent with current practice shifts on the Texas coast.
- Any tube use must budget for maintenance and for clear navigational marking.

- Monitoring should include crest surveys, incident logs for vessel related damage, and focused bathymetry at gaps and terminations to track scour and flanking.
- If access and costs allow, stone sills at the highest energy locations provide a more durable baseline for long term protection while still allowing habitat features in the lee.

Figure 10.Map showing the general area for the site visit near Galveston, Texas. Magenta lines indicate the locations of geotube deployments visited (including a reef ball deployment in the southwest of the map).

Figure 9. Close-up photograph of the material and growth on a textile geotube deployed near Hoeckers Point in West Bay, Galveston.

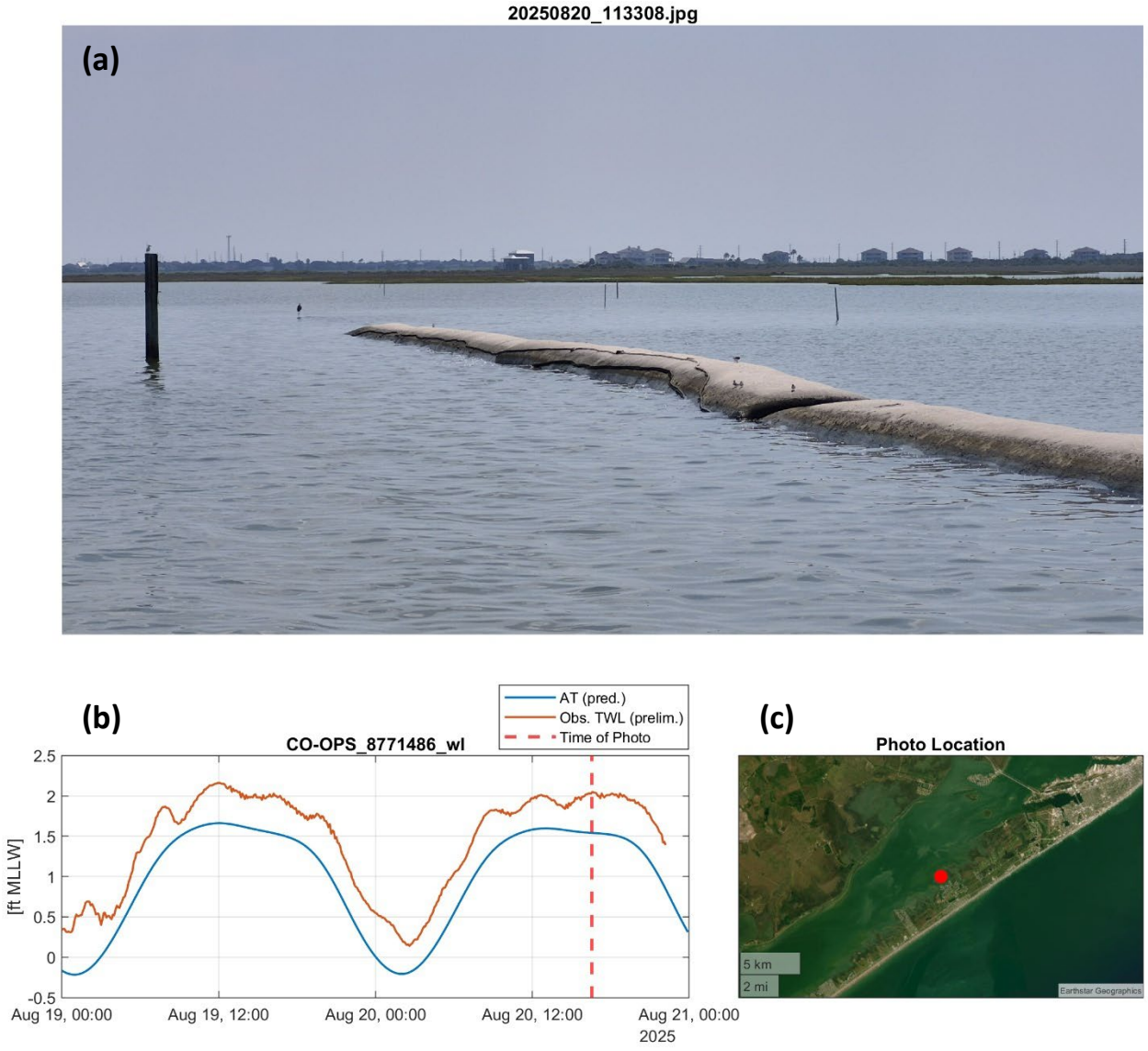

Figure 11. (a) Geotubes deployed near Hoeckers Point in West Bay, Galveston, (b) predicted tide and observed water levels at the time of the photograph and (c) a map showing the location of the photograph.

2.4 Numerical models

2.4.1 FVCOM

The Finite Volume Coastal Ocean Model (FVCOM Chen et al., 2003) It is a three-dimensional, primitive equation ocean model which solves equations describing the evolution of momentum, continuity, temperature, salinity, and density in coastal oceans and estuaries. FVCOM allows for the efficient horizontal discretization of large model domains by using unstructured meshes comprised of triangular elements. This allows for seamless transitions between high resolution near complex coastal geometries and shallow water and lower resolution offshore where processes are slower-varying, thereby optimizing computational cost. The model uses the σ-coordinate (terrain following) vertical scheme.

In this study, results from an existing FVCOM configuration developed by Ralston et al. (2017) are used to provide input data to the core sediment transport model described in Section 2.1.2. The model has been calibrated and validated, and successfully applied to investigations in the Connecticut River previously (e.g Yellen et al., 2017). Figure 12 shows the mesh nodes colored by depth in the FVCOM model of Ralston et al. (2017), with the study site annotated.

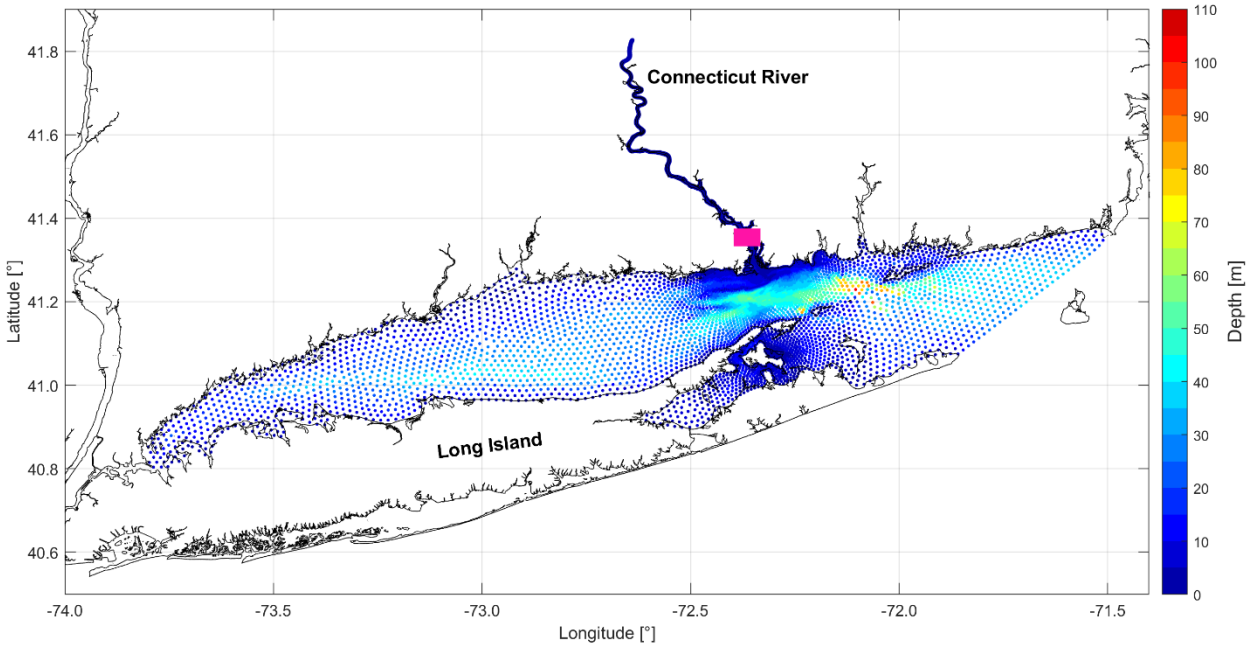

Figure 12. FVCOM model mesh nodes coloured by depth and the study domain at Essex, CT, highlighted by the magenta box.

2.4.2 Delft3D FLOW

Delft3D FLOW (D3D: Lesser et al., 2004) It is a three-dimensional primitive equation ocean model that solves the unsteady Reynolds-averaged Navier-Stokes equations. D3D has been extensively validated (Elias et al., 2000; Gerritsen et al., 2008; Roelvink & Van Banning, 1995) and has been deployed in similar contexts across the United States (e.g. Elias & Hansen, 2013; Georgiou et al., 2024; van der Wegen et al., 2017; van Rijn et al., 2025; Wang et al., 2023).

For this project, a D3D configuration was built from scratch to serve as the core of the sediment dynamics and erosion intervention experiments. The model uses a regular, curvilinear mesh and is deployed here in depth-averaged mode due to the shallow domain.

2.4.2.1 Mesh, Digital Elevation Model, and Virtual Envirotubes

The regular, curvilinear mesh D3D model mesh was constructed in the RGFGRID software application from Deltares. Horizontal resolutions ranging from 15-20 m near the open boundaries in the river channel to ~ 6 m owing to local refinement near the SE tail of Thatchbed Island. A digital elevation model (DEM) referenced to the North American Vertical Datum of 1988 (NAVD88) was constructed by combining data from the Coastal National Elevation Database (CoNED; U.S. Geological Survey, 2018) for areas below the NAVD88 with Light Detection and Ranging (LiDAR) data from the Connecticut Statewide LiDAR project for areas above the NAVD88. The coastline, which appears in figures throughout the report, is defined by the 0 m NAVD88 contour from the LiDAR data. The model mesh and bathymetry is shown in Figure 13.

In addition to the state LiDAR data, engineering drawings previously developed by Docko Sound Engineering Associated LLC and supplied to CIRCA by the Town of Essex Ad Hoc Committee – Thatchbed Island - were consulted for additional detailed elevation information specific to the Island. The digitized drawing is shown in Figure 14. In particular, the mean high and low water (MHL, MLW) contours from the drawings, as well as the 1 and 2 ft elevation contours, were digitized in GIS software for incorporation into the model DEM. The position of a rock pile (a previous erosion control intervention) was also digitized for use in the model. The contour elevations were converted to the model datum (NAVD88) and used in the final interpolation of the model DEM. Figure 15 depicts the various elevation data sources used to define the configuration of Thatchbed Island in the sediment model.

Envirotubes were modelled using the thin dam feature in Delft3D. Thin dams are barriers of infinitely small width, which prohibit exchanges between adjacent cells without affecting the total wet area or volume

(Deltares, 2020). The thin-dam feature in Delft3D is not material-specific to EnviroTube. In other words, the modeled reductions in bed shear stress and the resulting erosion–accretion patterns arise from the geometry, crest height relative to tides, and flow impedance of a continuous shore-parallel barrier are in the tested configurations, not the material it is made of. Therefore, the predicted benefits would be expected from any structure that achieves the same hydrodynamic effect (i.e., a geotextile tube array, low-crested rock breakwater, or a comparably performing living-shoreline sill), subject to design details that were not resolved in this study (porosity, surface roughness, overtopping behavior, structural stability under ice/boat-wake impacts, and long-term operation). Two thin dam files were developed to represent

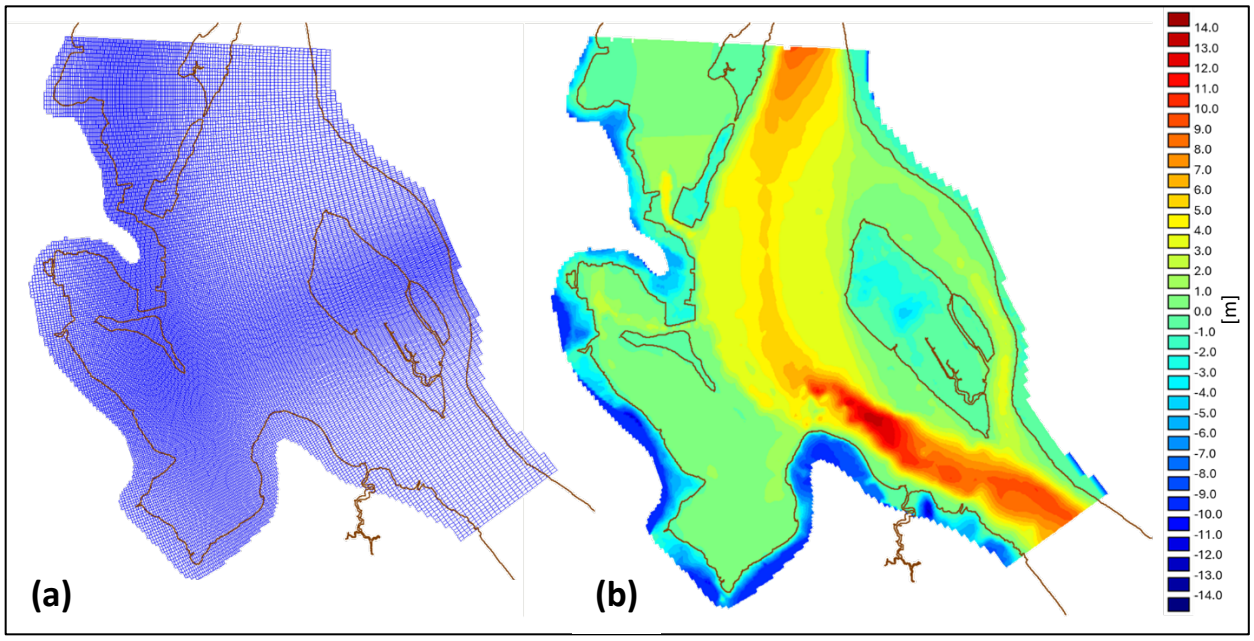

Figure 13. Delft3D model grid showing higher resolution near Thatchbed Island (a) and bathymetry (b). The coastline shown in these maps is the 0 m NAVD88 contour extracted from State LiDAR.

two possible Envirotube deployment configurations. Configuration 1 is a larger deployment which extends from the southeastern tail of the Island to the rock pile to the southeast. Configuration 2 is a smaller deployment designed as an alternative to, and a more limited test than, Configuration 1. In both cases, the model bathymetry was adjusted such that the elevation between the Island and the virtual Envirotubes was set to 3 ft MLW NAVD8 to represent backfill. Figure 12 shows the Envirotube configurations and corresponding model representations, including the backfill, which is shown as a difference with respect to the control bathymetry.

Figure 14. Engineering drawings from which additional bathymetric information was incorporated into the Delft3D model DEM.

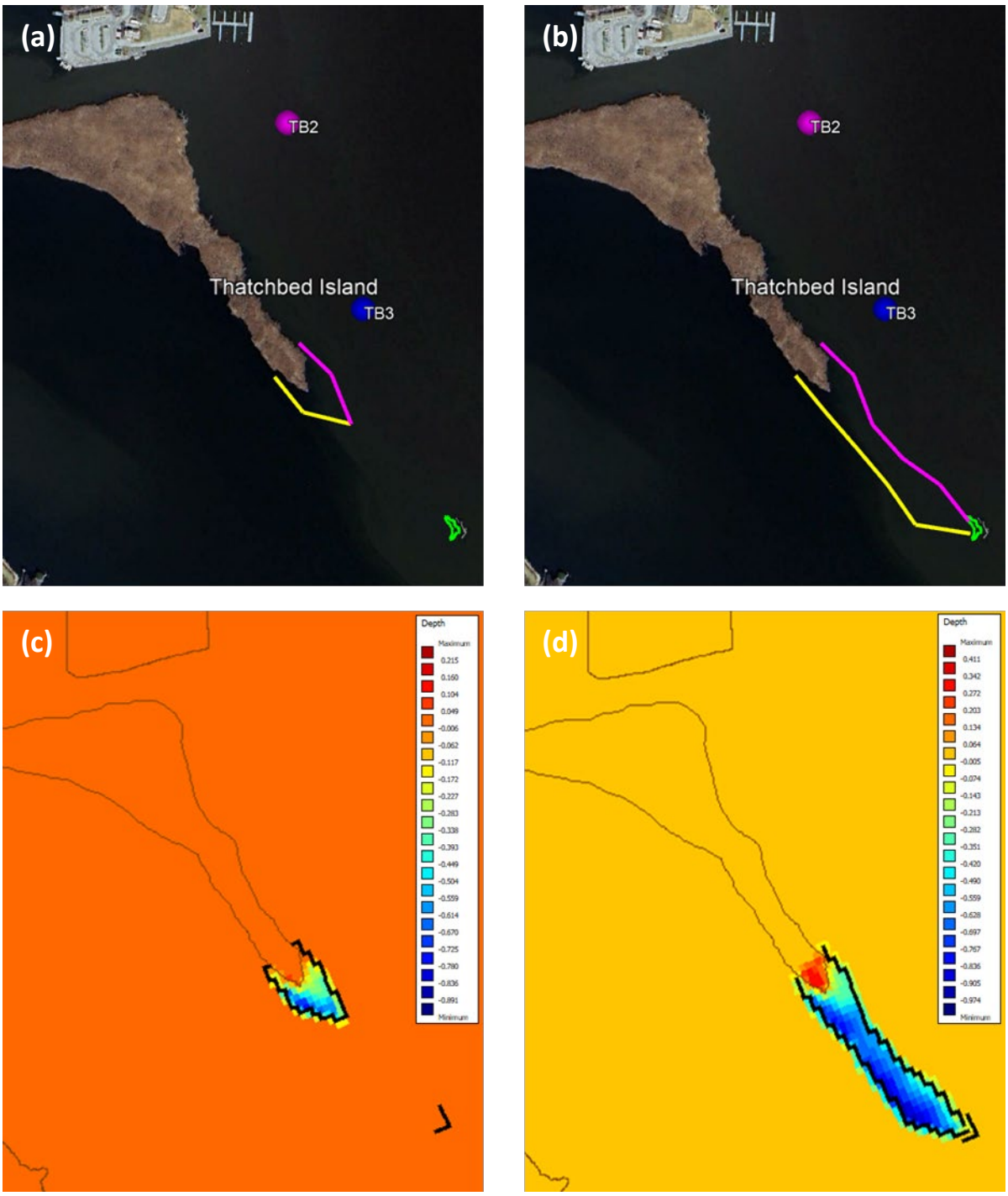

Figure 15. Potential Envirotube configurations 1 (larger deployment, panel b) and 2 (smaller deployment, panel a). Panels (c-d) show corresponding visualizations of the thin dam definitions in the model, with the backfill indicated as the difference from the natural bathymetry.

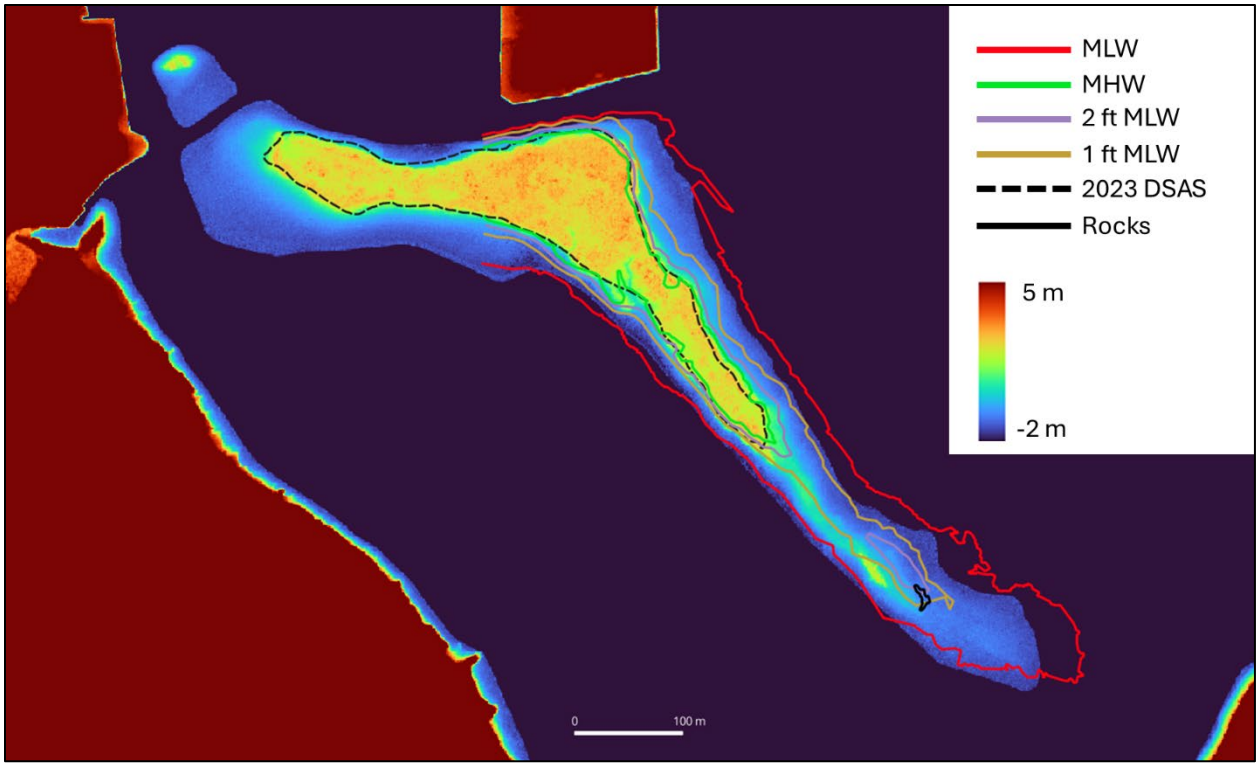

Figure 16. A map of Thatchbed Island showing the synthesizing of various sources of elevation information in QGIS for the representation of the island in the Delft3D model DEM. The shading represents the state LiDAR. The MLW, MHW, 1 ft, 2 ft contours were extracted from the digitized engineering drawings shown in Figure 6. The 2023 island outline is from the DSAS.

2.4.2.1 Sediment distributions

A 5 m layer of sediment above the non-erodible bed was stipulated in the model. This layer is comprised of two sediment classes; a sand class and a mud class as illustrated in the conceptual sketch in Figure 16. The two classes have different initial spatial distributions, based on an interpolation of the sediment samples collected in-situ (Figure 17, 18). Sediment characteristics applied to the two classes as required by the model are listed in Table 1 and Table 2.

Table 1. Parameter settings applied to sand (non-cohesive) class sediment in the D3D model.

Parameter	**Unit**	**Value/File**
Specific density	kg m^{-3}	2650
Median diameter (D_{50})	m	3.4027×10^{-4}
Dry bed density	kg m^{-3}	1600
Initial layer thickness at bed	m	#sand_layer_thick.sdb#
Diameter scaling factor	–	1.0
Reference density for hindered settling	kg m^{-3}	1600
Suspended-size dependence switch	–	0

Table 2. Parameter settings applied to mud (cohesive) class sediment in the D3D model.

Parameter	Unit	Value / File
Specific density	kg m^{-3}	2650
Salinity for saline settling velocity	ppt	0
Settling velocity (fresh water)	m s^{-1}	1.0×10^{-4}
Settling velocity (saline water)	m s^{-1}	5.0×10^{-4}
Critical shear stress for sedimentation	N m^{-2}	0.25
Critical shear stress for erosion	N m^{-2}	0.30
Erosion parameter	kg m^{-2} s^{-1}	1.0×10^{-4}
Dry bed density	kg m^{-3}	700
Initial layer thickness at bed	m	#mud_layer_thick.sdb#
Diameter scaling factor	–	1.0
Reference density for hindered settling	kg m^{-3}	1600
Suspended-size dependence switch	–	0

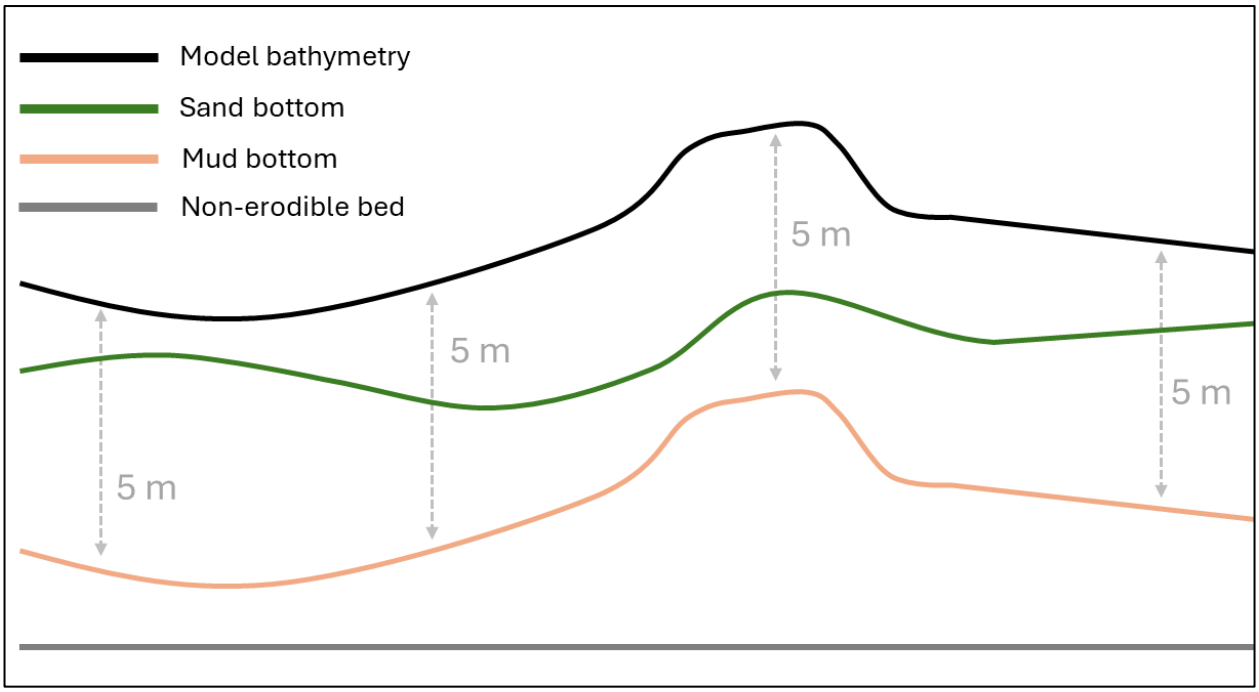

Figure 17. Conceptual sketch of the cross-sectional distribution of the two sediment classes used in the erosion simulations.

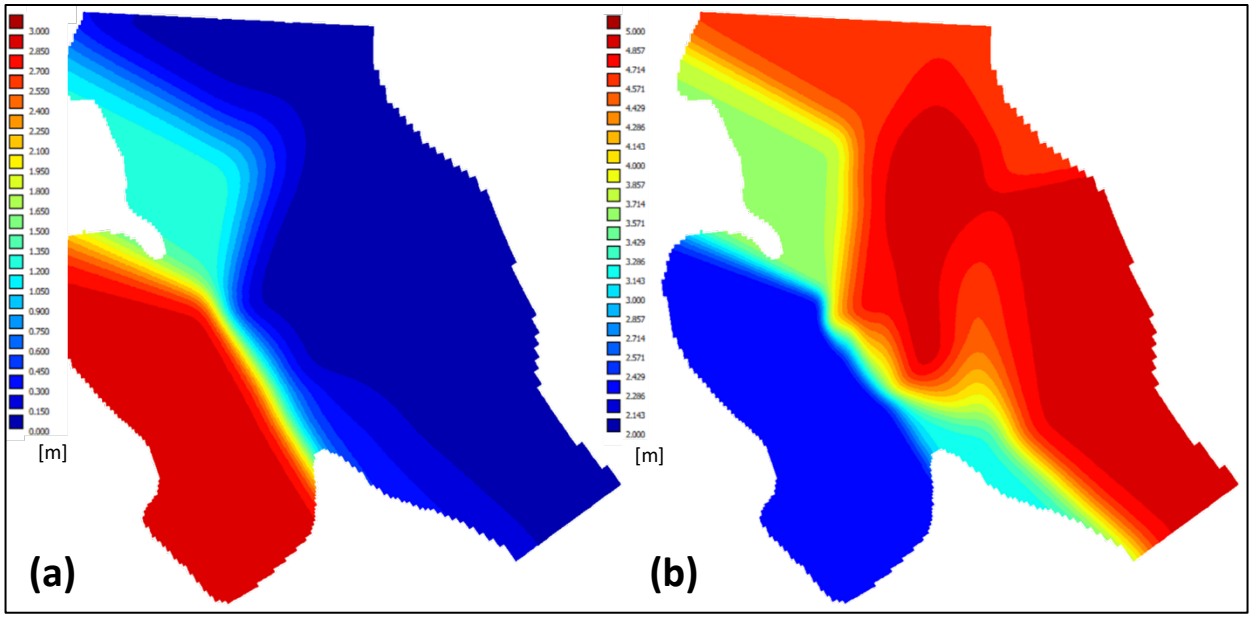

Figure 18. Horizontal distribution of initial sediment layer thickness for the mud (a) and sand (b) sediment classes.

2.4.2.2 Simulation Periods

Three simulation periods, referred to as P1-P3, were defined. These periods were defined based jointly on the availability of input data (see *2.4.2.3 Surface and Boundary Forcing*) from the large-scale FVCOM model of Ralston et al. (2017) and to ensure that a variety of forcing conditions were considered. To place river velocities and tidal conditions during simulation periods P1-3 in context, Figure 19 shows the three simulation periods as annotations on probability density distributions and time series plots for 2010-2024 from USGS streamflow and water level gauges at Thompsonville and Essex respectively.

Durations of the FVCOM simulations used as input data to the D3D model were different. Thus, in order to achieve a standard set of three 15-day simulations (to allow for a two-week period after discarding the first day for model spinup), the forcing from FVCOM simulations for periods P1 and P3 were artificially lengthened. This was achieved by searching each forcing signal for a window *W* in which the magnitude and derivative were similar to those shortly prior to the end of the signal. The portion of the time series following *W* was then spliced (with some smoothing) to the natural end of the signal, resulting in an artificially lengthened but still-physically realistic time series spanning 15 days.

Since morphological changes occur on timescales which are typically several orders of magnitude larger than those of hydrodynamic processes, it is often impractical to detect noticeable changes due to erosion and sedimentation in high-resolution hydrodynamic simulations, which, given computational constraints,

cover periods of hours to weeks. To overcome this, the Delft3D allows for a so-called Morphological Scale Factor (Deltares, 2020) to be defined. MSF is a scalar multiplier applied to the sediment continuity equation, thereby multiplying erosion and deposition fluxes at each computational step. This allows for morphological changes to the model bed to be accelerated. This non-physical multiplier should be used with caution. Morgan et al. (2020) provide a comprehensive investigation of the implications of the MSF, suggesting that usage is best restricted to short-term and/or smaller model domains, both of which apply to the D3D model used in this study. Notwithstanding, for each model experiment, we first ran the simulation with MSF = 1 (the natural, or control case) to ensure stability and facilitate the diagnosis of any artefacts introduced by the use of the MSF, followed by a simulation with MSF = 25. This value was selected to be well within the ranges tested by Morgan et al. (2020) of 5 to 50, and to represent loosely one year's worth of fortnightly tidal cycles.

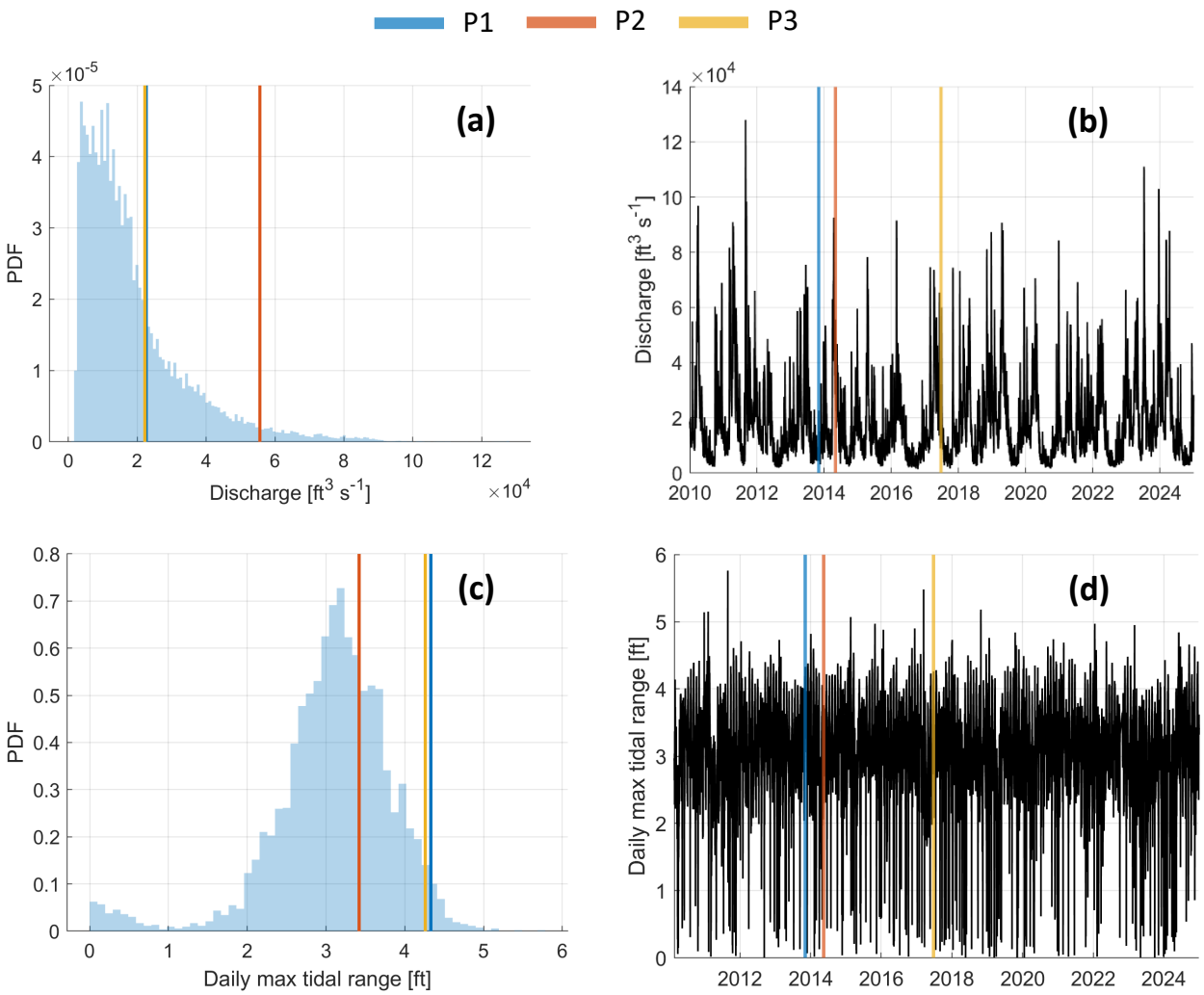

Figure 19. Probability density distributions and time series of discharge (a-b) and tidal range (c-d) from USGS gauges at Thompsonville and Essex from 2010-2024 respectively. Vertical lines represent simulation periods P1-P3 and place the simulations in context in terms of the magnitude of their forcing.

2.4.2.3 Surface and Boundary Forcing

Hourly 10 m wind and mean sea level pressure forcing derived from the ERA5 reanalysis product (Hersbach et al., 2020) was applied to the D3D model. To ensure that the meteorological forcing remained physically consistent with the extended hydrodynamic forcing at the open boundaries (see), the wind and pressure signals were extended using the same methodology as was used to extend the velocity and water level forcing signals (see *2.4.2.2 Simulation Periods*). Figure 20 shows the time series of mean sea level pressure and wind applied to the model during simulation period P1.

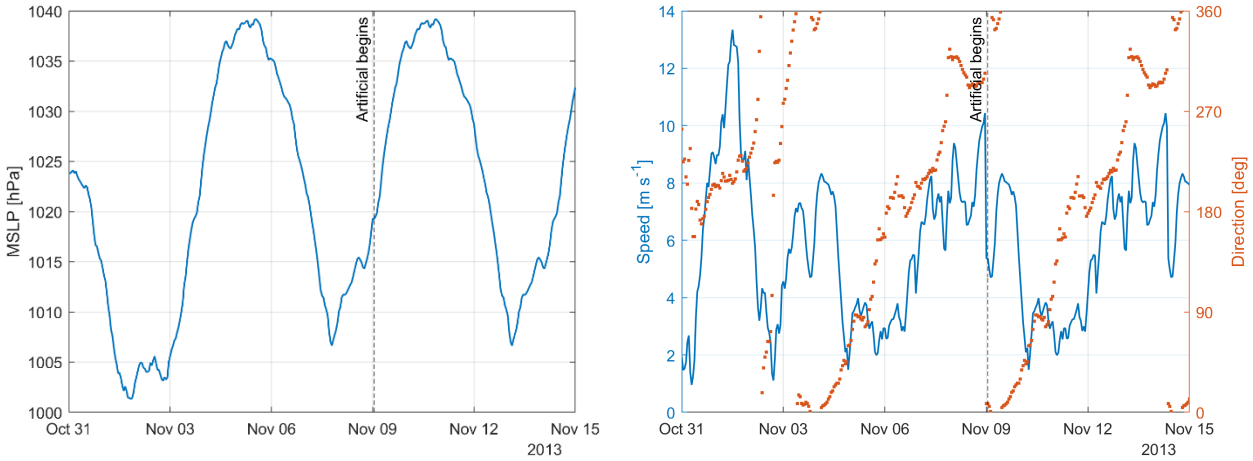

Figure 20. ERA5 atmospheric pressure (a) and wind (b) forcing applied to the sediment simulations for simulation period P1. Plots for P2 and P3 can be found in Appendix E. Supplementary Figures.

Depth-averaged velocity signals, extracted from the model results of Ralston et al. (2017), were imposed along the 5 sections defining the northern open boundary in the river channel. Figure 21 shows the time series of cross-boundary forcing applied to the D3D model for simulation period P1. The figure is annotated to show the point at which the time series is artificially extended, as explained in *2.4.2.2 Simulation Periods*.

In addition to velocity boundary conditions at the northern boundary, total water level (TWL) boundary forcing was applied to the D3D southern open boundary. TWL signals were also extracted from the model results of Ralston et al. (2017) and applied to each of 5 boundary sections, into which the boundary was divided. Figure 22 show the time series of the TWL forcing applied to the D3D model for simulation period P1. The figure is annotated to reflect the artificial extension of the time series, as explained in *2.4.2.2 Simulation Periods*.

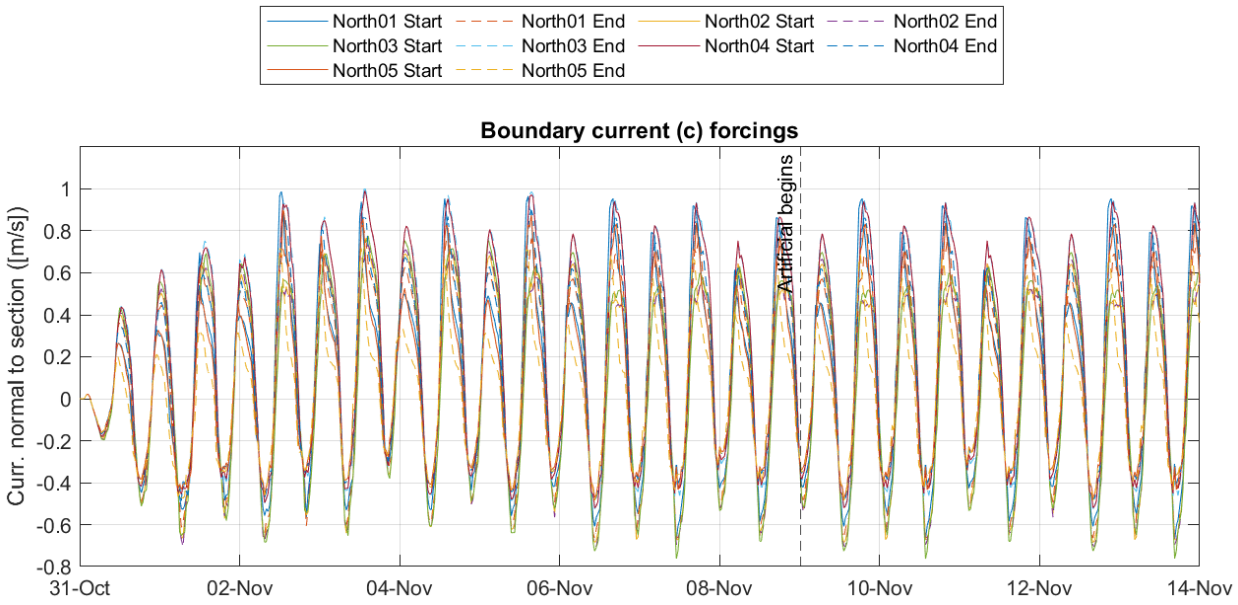

Figure 22. Depth-averaged velocity forcing imposed on each of the sections (differentiated by color, as per legend) at the upstream open boundary. Positive velocities represent flow into the domain (downstream) and negative velocities represent flow out of the domain (upstream). Shown here is the forcing for simulation period P1. Plots for P2 and P3 can be found in Appendix E. Supplementary Figures.

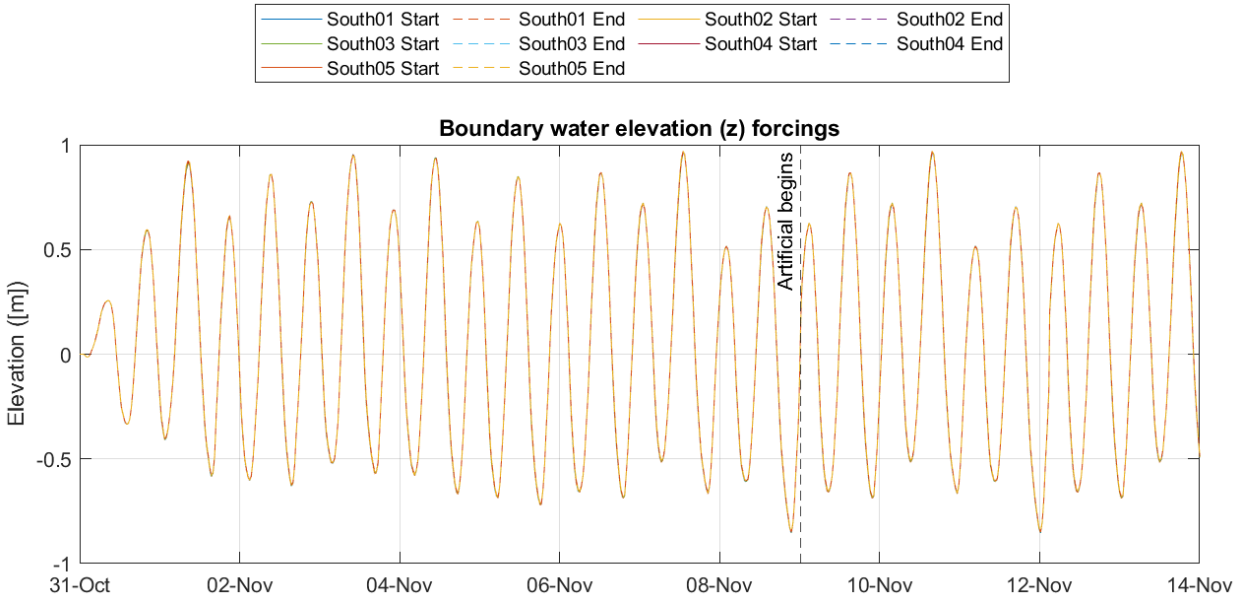

Figure 21. Total water level elevation forcing relative to NAVD88 imposed at each of the downstream open boundary sections. Shown here is the forcing for simulation period P1. Plots for P2 and P3 can be found in Appendix E. Supplementary Figures.

3. Model Results and Discussion

3.1 Model Calibration

Model calibration was conducted by comparing key modelled and measured distributions. Input (forcing) data coverage for the D3D sediment model was unavailable for the period during which measurement data were collected. Thus, modelled and measured distributions are not expected to match as closely as if they were temporally coincident and were compared to ensure correct orders of magnitude and variability in the D3D model Figure 23. The model was iteratively tuned via a series of simulations in which one parameter was varied at a time, to arrive at a set of parameter settings for use in the sediment simulations. Initial comparisons revealed velocities to be too high in the channel (a consequence of the boundary forcing), and thus space-varying and anisotropic bottom roughness and horizontal eddy viscosity settings were used to reduce along-channel flow velocities without compromising agreement in shallower regions near Thatchbed Island. Following calibration, the D3D model produced bed shear stresses, velocities and water level variability in good agreement with observed distributions for similar seasonal time periods. Table 3 summarizes the final parameter settings.

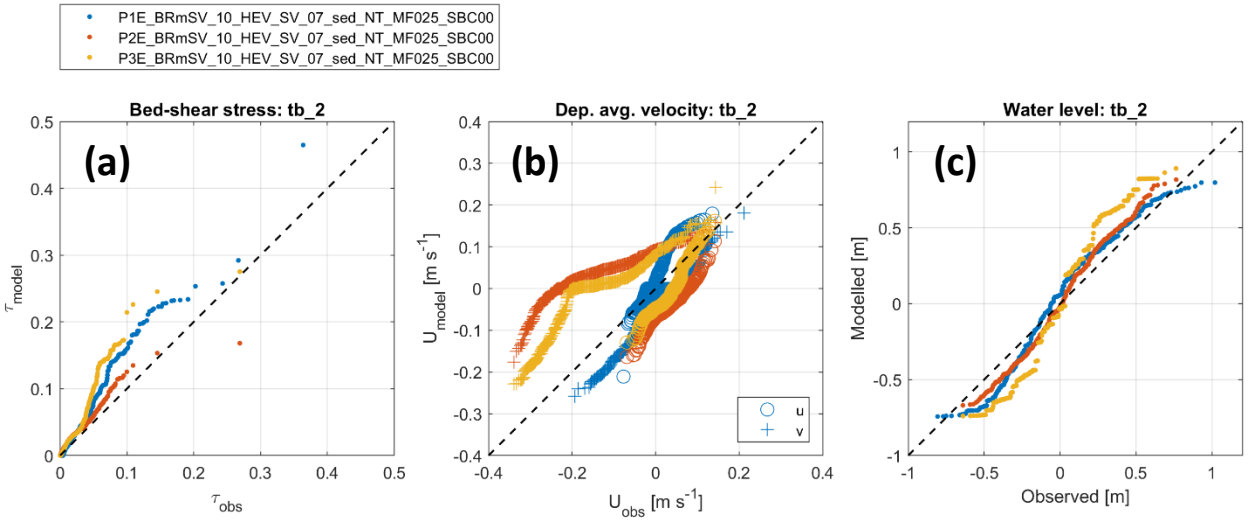

Figure 23. D3D model quantile-quantile calibration curves. Colors indicate different simulations periods. Panels (a-c) show bed shear stress, depth averaged velocity and total water levels respectively, at location tb_2, in the shallows immediately east of Thatchbed Island.

Table 3. Bottom roughness and horizontal eddy viscosity calibration settings.

Parameter	Value (u-direction)	Value (v-direction)	Notes
Bottom roughness	0.032 (channel), 0.021 (shallows)	0.040 (channel), 0.019 (shallows)	Anisotropic Manning's formulation
Horizontal eddy viscosity	0.5 $m^2 s^{-1}$ (shallows)	3.2 $m^2 s^{-1}$ (channel)	Space-varying

3.2 Erosion and Sedimentation

Modelled flow around the southeastern tail of Thatchbed Island was found to be sensitive to the presence of, and deployment configuration of the virtual Envirotubes. Figure 24 shows a snapshot example of depth averaged velocities during flooding and ebbing tides, in which the circulation pattern near the southeastern tail of the Island has been modified due to the presence of the virtual Envirotubes.

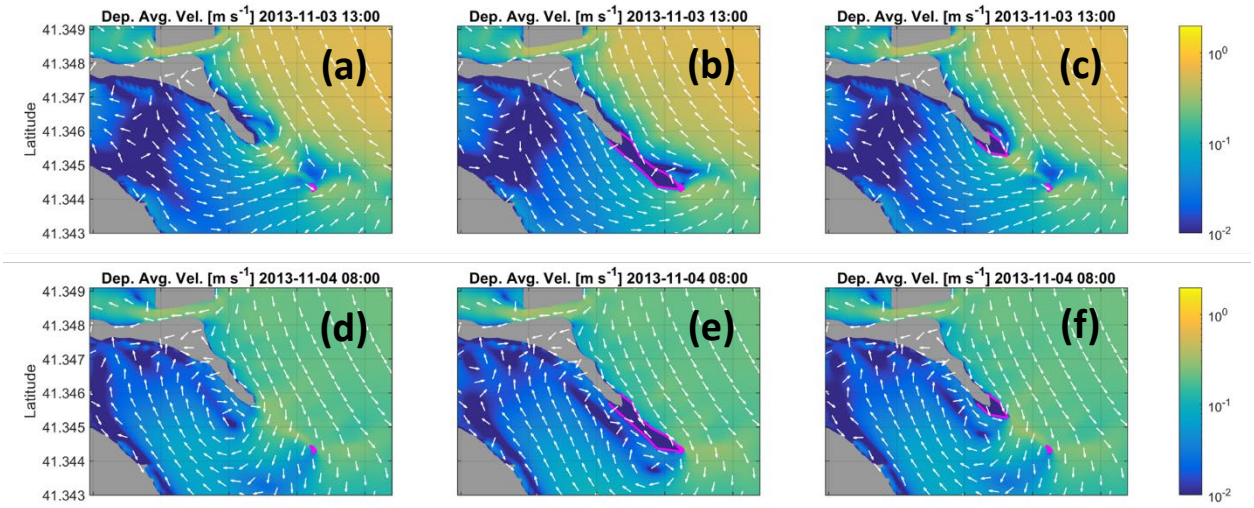

Figure 24. Depth averaged velocity fields near Thatchbed Island during flood (a, b, c) and ebb (d, e, f) tide. Panels (a, d) show the control simulations with no Envirotubes, whilst panels (b, e) and (c, f) show simulations with Envirotube Configurations 1 and 2 respectively.

Consequent differences in erosion and sedimentation around Thatchbed Island are highlighted by comparing cumulative changes to the bed level (Figure 25). For each simulation period, the control simulation (panels a, d, e: no Envirotubes) is presented alongside corresponding results from simulations with Envirotube Configuration 1 (panels b, e, g: the larger deployment) and Configuration 2 (panels c, f, i: the smaller deployment).

Across all three time periods (forcing regimes), a narrow, shore-hugging high-velocity core wraps around the SE tail during both flood and ebb tides in the control runs (no Envirotubes), raising bed shear there and driving persistent erosion near the tip of Thatchbed Island. The introduction of Envirotubes causes flow to be deflected offshore, producing a sheltering the area behind the deployments and reducing erosion. The smaller deployment (Configuration 2) generates partial protection: the velocity jet reconverges tightly at the downstream tube end, yielding localized, shoreline-adjacent scour tongues. The larger deployment (Configuration 1) alters the flow more broadly, yielding a wider, steadier wake and pushing erosive reconvergence further from the Island.

These results are shown again in a series of difference maps in Figure 26, compiled by subtracting the cumulative changes in each of the Envirotube simulations from the control simulation. Blue areas indicate zones where the bed is higher (where Envirotubes led to reduced erosion or enhanced deposition along the protected shoreline) whereas red areas mark zones where the bed is lower, reflecting increased erosion or reduced deposition, typically concentrated at the downstream tube ends. The larger deployment produces larger relative differences (i.e. more noticeable protection) than the smaller deployment, with clear patterns of erosion emerging immediately southeast of the smaller deployment's termination. It should be noted that, whilst the difference maps suggest that the bed level beyond the rock pile (without Configuration 1) and between the Envirotubes and rock pile (without Configuration 2) would remain higher (blue) in the absence of Envirotubes, cross-referencing with Figure 26 confirms that this is due to slightly enhanced erosion, rather than enhanced deposition. This is likely due to the deflection of the local acceleration of channel velocities by the Envirotubes, and is likely to occur wherever the intervention terminates. Notwithstanding, the magnitude remains small, on the order of 10 cm over the 25 two-week cycles.

Period-to-period variations mirror changes in hydrodynamic forcing. Under the comparatively moderate regime of P2, the sheltered wake and end-effects are muted. During P1 and P3, the contrasts sharpen with baseline erosion intensifying and end-scour associated with Configuration 2 becomes most pronounced. Configuration 1 remains the most effective across all regimes, maintaining shoreline deposition even during relatively high-forcing conditions. The relative differences between different deployment configurations are most pronounced during periods of energetic forcing near the Island (e.g. P1 and P3), while during periods of relatively weak forcing (e.g. P2), the influence of the Envirotubes (and the differences between configurations) is markedly less noticeable.

Finally, potential far-field impacts were investigated, and revealed to be negligible, with impacts on erosion and sedimentation confined almost exclusively to the area near the southeastern tail of Thatchbed Island. Figure 27 shows a map of the cumulative bed changes for the broader domain for simulation Period P3, indicating the clear confinement of significant changes to the area around the interventions. Corresponding plots for P1 and P2 can be found in Appendix E. Supplementary Figures.

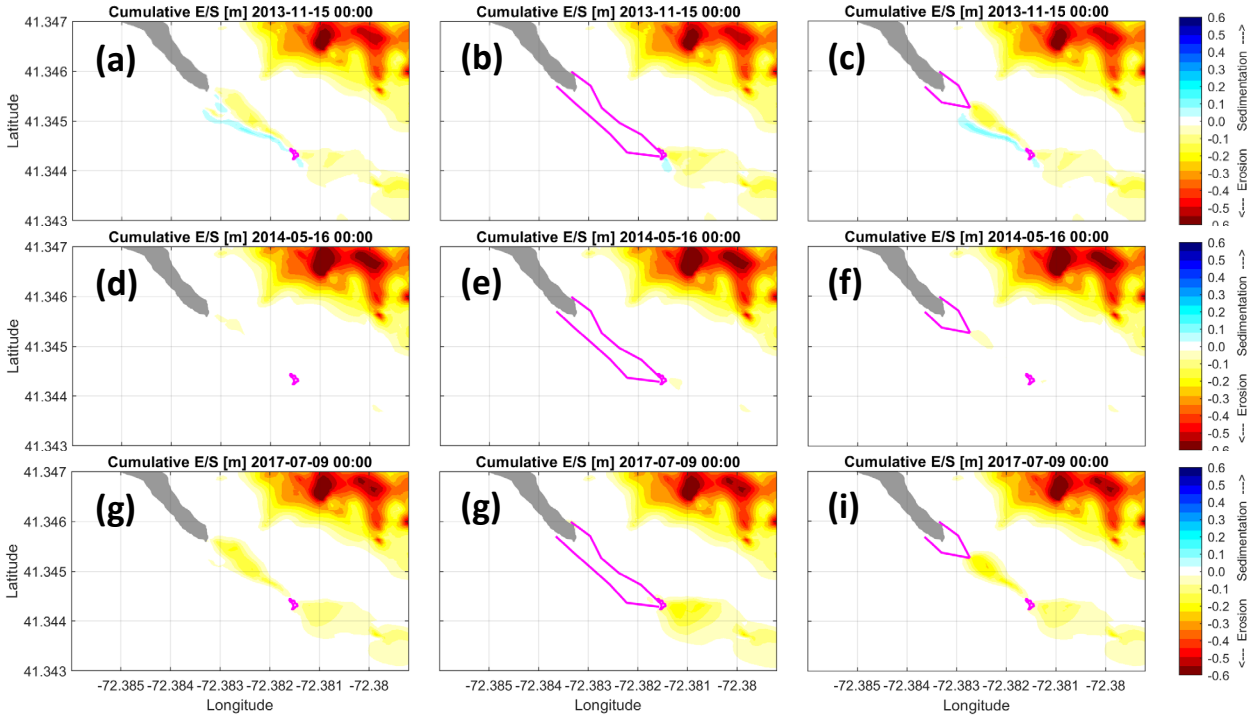

Figure 25. Spatial distribution of cumulative sedimentation (blue) and erosion (red) after 15 days and accelerated by a factor of 25. The southeastern tail of Thatchbed Island is visible in the top left portion of each panel. Panels are arranged such that rows (top-bottom) represent simulation periods 1-3 and columns (left to right) represent the configuration of the erosion interventions. Panels a, d, g (column 1) are the control simulations (no virtual Envirotubes deployed); panels b, e, g (middle column) are results with the larger Envirotube configuration and panels c, f, i (right column) are results with the limited virtual deployment.

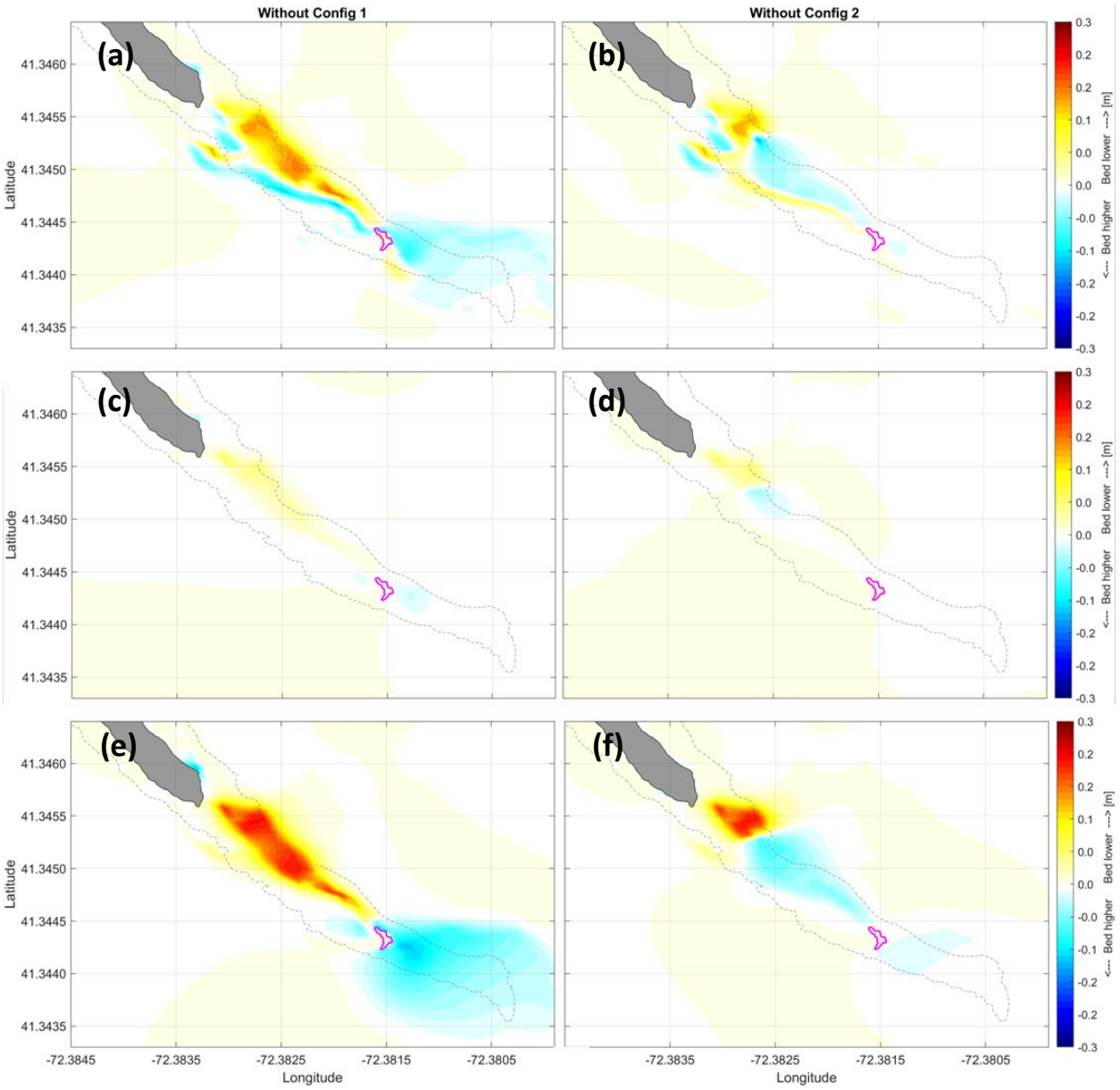

Figure 26. Relative difference in bed level in the absence of Envirotube larger configuration 1 (panels a, c, e) and smaller configuration 2 (panels b, d, f) for simulation periods 1-3 (rows). The southeastern tail of Thatchbed Island is visible in the top left portion of each panel. The historical outline of the Island (1991) from the DSAS is shown as a gray dashed line. The rock pile is shown in magenta.

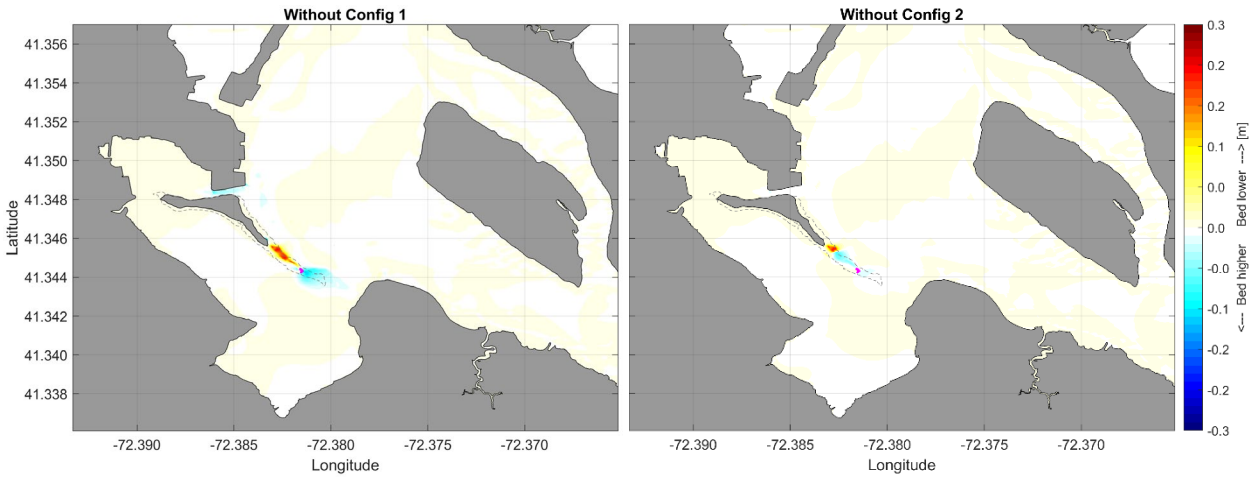

Figure 27. Relative difference in bed level in the absence of Envirotube larger Configuration 1 (panel a) and smaller Configuration 2 (panel b) over the broader domain, including the river channel, for simulation Period P3. The historical outline of the Island (1991) from the DSAS is shown as a gray dashed line. The rock pile is shown in magenta. Plots for P1 and P2 can be found in Appendix E. Supplementary Figures.

4. Conclusions and Recommendations

The team combined (i) historical shoreline-change analysis (1991–2023), (ii) two rounds of in-situ hydrodynamic and sediment observations targeting spring high-flow conditions, (iii) process-based numerical modeling (Delft3D) configured with site bathymetry and sediment mapping, and (iv) practitioner insights from field reconnaissance in Texas and structured interviews with long-term operators of geotextile-tube and alternative systems. This integrated approach was used to diagnose the dominant drivers of erosion at Thatchbed Island, test candidate shore-parallel barrier layouts digitally, and translate findings into implementable, operations-aware recommendations.

Shoreline change analysis demonstrates persistent net erosion of Thatchbed Island from 1991 to 2023 with the greatest mobility and land loss concentrated along the southeastern spit. Regression-based rates converge on a regional average retreat near 1.77 ft per year, with a high share of transects exhibiting statistically significant erosion. The spatial pattern is consistent with the island platform and with measured hydrodynamics and bed shear in the adjacent shallows.

Numerical model experiments represent the barrier as a hydraulically opaque, shore-parallel obstruction with a specified footprint and crest level; it does not resolve material-specific behaviors such as porosity, face roughness, or overtopping hydraulics. Modelling the impact of the Envirotube installations on erosion suggest that the interventions successfully displaced the erosive jet and fostered localized sediment

retention behind the Envirotubes. Scenario tests indicate that a continuous, shore-parallel barrier placed along the tail reduces bed shear stress in its lee, displaces the erosive jet offshore, and promotes localized sediment retention behind the alignment. The magnitude and footprint of bed-level protection appear to be jointly governed by forcing strength and deployment geometry. A similar level of protection should be attainable with any structure that delivers the same flow reduction. Final selection among alternatives should consider those material-specific performance and maintenance differences in addition to the hydrodynamic results reported here.

Site visits and interviews with long-term practitioners suggest that geotextile tube systems can attenuate waves and promote accretion in calm or moderately energetic settings. However, durability depends on selecting the correct crest, filling with sand, implementing robust toe and end treatments, and maintaining consistency. The primary failure modes reported are driven by human interaction, including wakes, anchoring, prop strikes, and vandalism, with ultraviolet degradation as a chronic stressor. Several legacy installations have been capped or replaced with rock after years of patching. Navigation safety and clear marking are recurring concerns, particularly where crests sit near typical water levels. Feedback from the discussions emphasizes that any near-term use of geotextile containment at Thatchbed Island must be paired with a credible operations and maintenance program and financial assurance.

Recommendations may include:

1) Adopt a phased approach that begins with a limited-length pilot at the southeastern tail to verify local performance, construction logistics, and maintenance burden before considering a longer alignment. Use the same transect geometry and statistics from the shoreline analysis as the basis for the before-and-after comparison.
2) May use stone sills at the highest energy and highest traffic margins and reserve geotextile containment, if used at all, for lower energy segments where access limits heavy equipment and where vessel interaction risk can be controlled. Where geotextile containment is used, specify a sand fill and a scour mat at the toe, along with detailed end treatments to resist flanking.
3) Document crest, backfill platform, and gap elevations in datum and control them with construction surveys.
4) Establish an exclusion zone with day boards, aids to navigation as appropriate, and signage that communicates no mooring, no landing, and gear exclusion. Include seasonal inspection for

damage related to wakes, debris, and ice. Coordinate with harbor management to incorporate the zone into local notices.

5) Require an operations and maintenance plan that covers routine inspection frequency, patching methods, criteria for section replacement, debris retrieval, and winter and post-storm inspections. Include a contingency stating what will happen if recurring damage exceeds defined thresholds.
6) Define quantitative success metrics in advance, such as minimum positive change in backfill platform elevation, a target reduction in modeled or measured bed lowering adjacent to the tail, and vegetation establishment thresholds on the platform to help with monitoring.

These recommendations can help manage operational risks by documenting project outcomes to ensure a durable solution.

5. References

Chen, C., Liu, H., & Beardsley, R. C. (2003). An Unstructured Grid, Finite-Volume, Three-Dimensional, Primitive Equations Ocean Model: Application to Coastal Ocean and Estuaries. *Journal of Atmospheric and Oceanic Technology*, *20*, 159–186. https://doi.org/https://doi.org/10.1175/1520-0426(2003)020%3C0159:AUGFVT%3E2.0.CO;2

Deltares. (2020). *Delft3D FLOW – Simulation of multi-dimensional hydrodynamic flows and transport phenomena, including sediments, User Manual*. Deltares.

Elias, E. P. L., & Hansen, J. E. (2013). Understanding processes controlling sediment transports at the mouth of a highly energetic inlet system (San Francisco Bay, CA). *Marine Geology*, *345*, 207–220. https://doi.org/10.1016/j.margeo.2012.07.003

Elias, E. P. L., Walstra, D. J. R., Roelvink, J. A., Stive, M. J. F., & Klein, M. D. (2000). Hydrodynamic validation of Delft3D with field measurements at Egmond. *Coastal Engineering 2000 - Proceedings of the 27th International Conference on Coastal Engineering, ICCE 2000*, *276*. https://doi.org/10.1061/40549(276)212

Georgiou, I. Y., FitzGerald, D. M., Sakib, M. M., Messina, F., Kulp, M. A., & Miner, M. D. (2024). Storm Dynamics Control Sedimentation and Shelf-Bay-Marsh Sediment Exchange Along the Louisiana Coast. *Geophysical Research Letters*, *51*(22). https://doi.org/10.1029/2024GL111344

Gerritsen, H., De Goede, E. D., Platzek, F. W., van Kester, J. A. T. M., Genseberger, M., & Uittenbogaard, R. E. (2008). *Validation Document Delft3D- FLOW, a software system for 3D flow simulations* (1.1). Deltares.

Hersbach, H., Bell, B., Berrisford, P., Hirahara, S., Horányi, A., Muñoz-Sabater, J., Nicolas, J., Peubey, C., Radu, R., Schepers, D., Simmons, A., Soci, C., Abdalla, S., Abellan, X., Balsamo, G., Bechtold, P., Biavati, G., Bidlot, J., Bonavita, M., … Thépaut, J. N. (2020). The ERA5 global reanalysis. *Quarterly Journal of the Royal Meteorological Society*, *June*, 1999–2049. https://doi.org/10.1002/qj.3803

Lesser, G. R., Roelvink, J. A., van Kester, J. A. T. M., & Stelling, G. S. (2004). Development and validation of a three-dimensional morphological model. *Coastal Engineering*, *51*(8–9), 883–915. https://doi.org/10.1016/j.coastaleng.2004.07.014

Morgan, J. A., Kumar, N., Horner-Devine, A. R., Ahrendt, S., Istanbullouglu, E., & Bandaragoda, C. (2020). The use of a morphological acceleration factor in the simulation of large-scale fluvial morphodynamics. *Geomorphology*, *356*. https://doi.org/10.1016/j.geomorph.2020.107088

Ralston, D. K., Cowles, G. W., Geyer, W. R., & Holleman, R. C. (2017). Turbulent and numerical mixing in a salt wedge estuary: Dependence on grid resolution, bottom roughness, and turbulence closure. *Journal of Geophysical Research: Oceans*, *122*(1), 692–712. https://doi.org/10.1002/2016JC011738

Roelvink, J. A., & Van Banning, G. K. F. M. (1995). Design and development of DELFT3D and application to coastal morphodynamics. *Oceanographic Literature Review*, *11*(42), 925.

Sealey, K. (2024). Woods and Waters. *Essex Land Trust Newsletter*, 1–8. https://essexlandtrust.org/wp-content/uploads/2024/06/Woods-Waters-Winter-2024-web.pdf

U.S. Geological Survey. (2018). *USGS EROS Archive - Digital Elevation - Coastal National Elevation Database (CoNED) Project - Topobathymetric Digital Elevation Model (TBDEM)*. U.S. Geological Survey.

van der Wegen, M., Jaffe, B., Foxgrover, A., & Roelvink, D. (2017). Mudflat Morphodynamics and the Impact of Sea Level Rise in South San Francisco Bay. *Estuaries and Coasts*, *40*(1), 37–49. https://doi.org/10.1007/s12237-016-0129-6

van Rijn, L. C., Geleynse, N., Perk, L., & Condon, D. (2025). Longshore Sediment Transport and Sediment Budgets, Southeast Florida Coast, U.S.A. *Journal of Coastal Research*, *41*(4). https://doi.org/10.2112/JCOASTRES-D-24-00070.1

Wang, N., Chen, Q., Hu, K., Xu, K., Bentley, S. J., & Wang, J. (2023). Morphodynamic modeling of Fourleague Bay in Mississippi River Delta: Sediment fluxes across river-estuary-wetland boundaries. *Coastal Engineering*, *186*, 104399. https://doi.org/10.1016/j.coastaleng.2023.104399

Yellen, B., Woodruff, J. D., Ralston, D. K., MacDonald, D. G., & Jones, D. S. (2017). Salt wedge dynamics lead to enhanced sediment trapping within side embayments in high-energy estuaries. *Journal of Geophysical Research: Oceans*, *122*(3), 2226–2242. https://doi.org/10.1002/2016JC012595

Appendices

A. Description of Model Configuration and Result Files

A1. Model Mesh and Topobathy Data

The model mesh file and accompanying enclosure files are *splines_02_refine_01.grd* and *splines_02_refine_01.enc*. Copies of these files are available in all simulation directories and are common to all experiments.

Topobathy files vary by Envirotube configuration, as they require different bathymetry data to reflect the different backfill distributions. Model topobathy files for the control, Configuration 1 and Configuration 2 experiments are *dep_thatch_09a.dep*, *dep_thatch_10a.dep* and *dep_thatch_11a.dep* respectively, with copies in each simulation directory.

A2. Model Results

Each simulation making up the experiment ensemble has a unique identifier based on parameter choices other configuration characteristics. The construction of the identifiers is explained below:

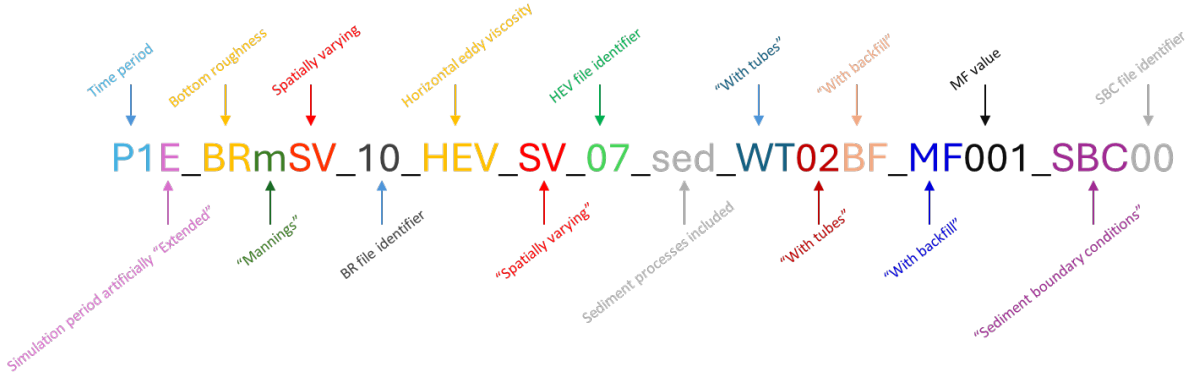

At the time of writing, simulation directories are archived on UConn CIRCA's model result archive on the Triton cluster at: */e1/CIRCA_modelling/Thatchbed_Island/<simulation_id>*

Raw model outputs include so-called map (2D) results files (trim-mdf_thatch.dat/def) and history (1D, at points of interest) files (trih-mdf_thatch.dat/def). Post-processed outputs in Matfile (.mat) format are also archived in */e1/CIRCA_modelling/Thatchbed_Island/postpro_data*, with filenames corresponding to simulation IDs.

C. Description of Site Visit Photographs and Supplementary Information

The full set of processed photographs taken during the site visit to Galveston, along with corresponding water level and geolocation information is available in the project archive at: *data\galveston_site_visit*

D. Supplementary Figures

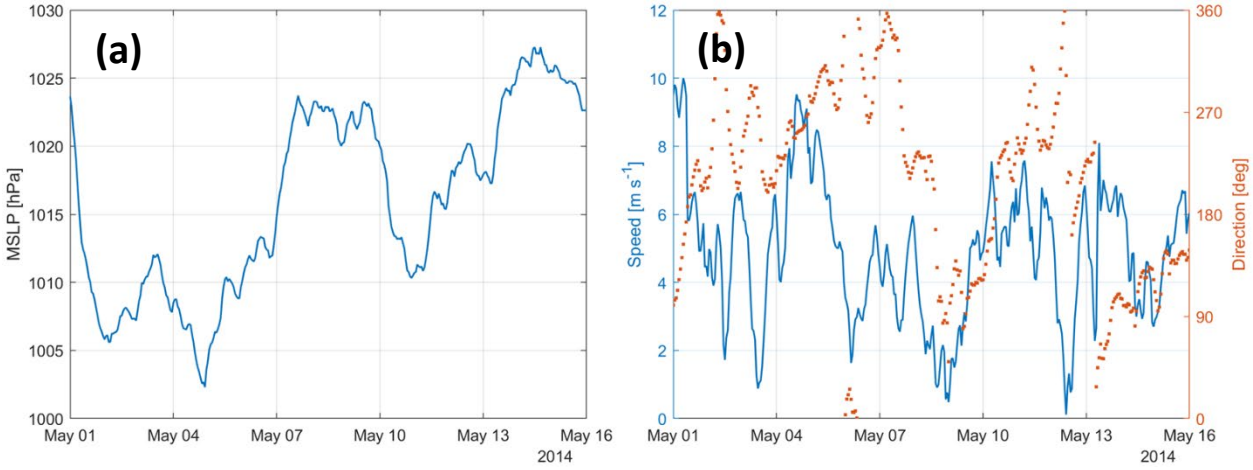

Figure S 1. ERA5 atmospheric pressure (a) and wind (b) forcing applied to the sediment simulations for simulation period P2.

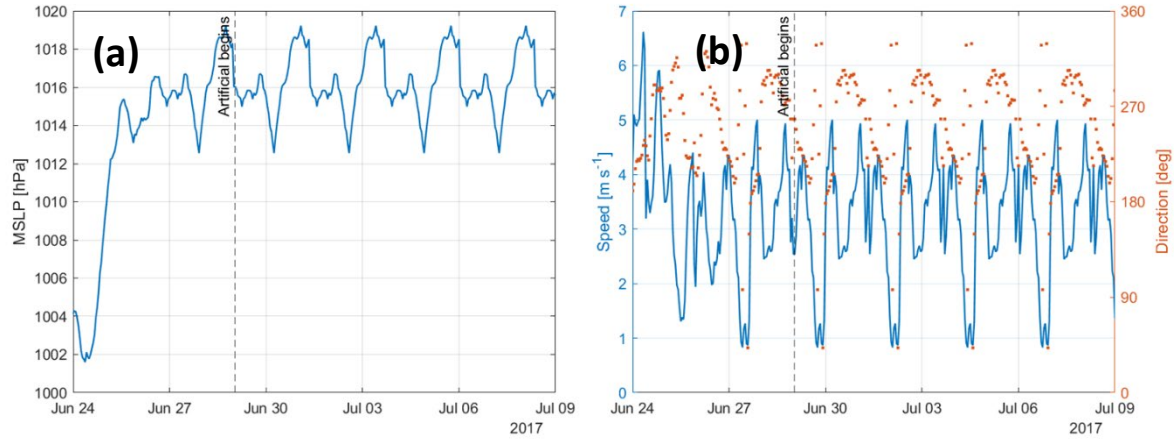

Figure S 2. ERA5 atmospheric pressure (a) and wind (b) forcing applied to the sediment simulations for simulation period P2.

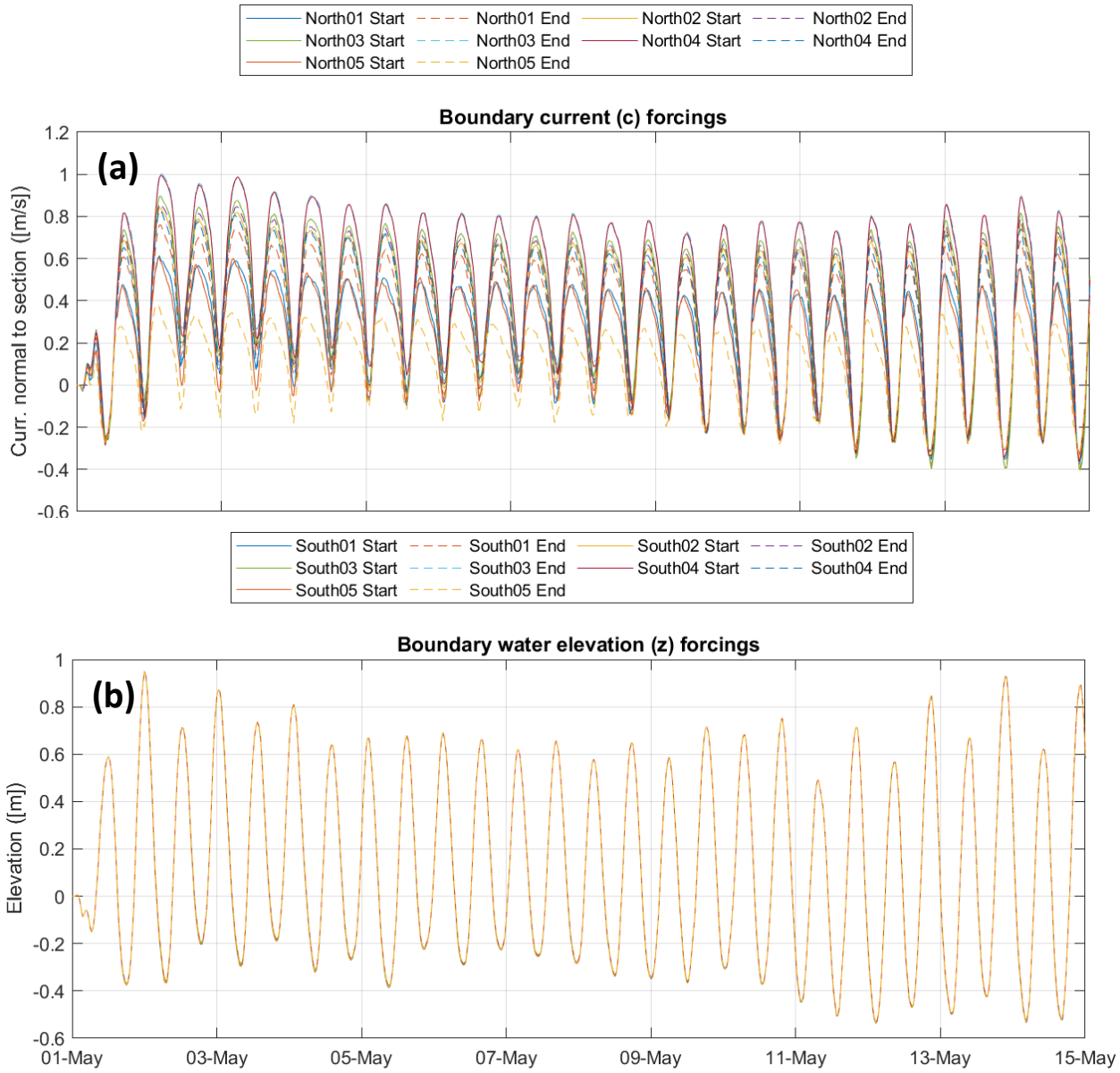

Figure S 3. Depth-averaged velocity (a) and total water level (b) forcing imposed on each of the sections (differentiated by color, as per legend) at the open boundaries for simulation period P2. Positive velocities in (a) represent flow into the domain (downstream) and negative velocities represent flow out of the domain (upstream).

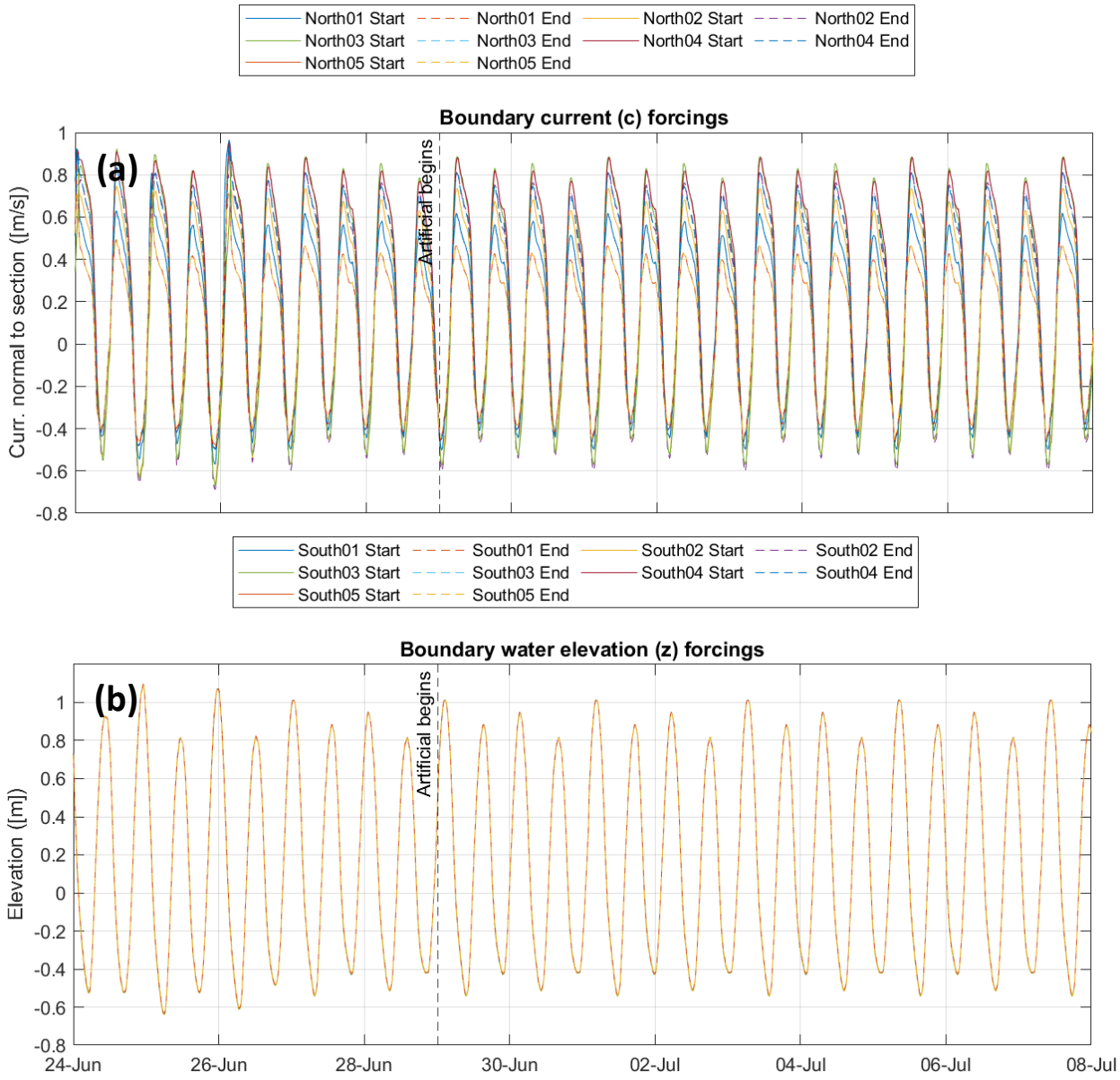

Figure S 4. Depth-averaged velocity (a) and total water level (b) forcing imposed on each of the sections (differentiated by color, as per legend) at the open boundaries for simulation period P2. Positive velocities in (a) represent flow into the domain (downstream) and negative velocities represent flow out of the domain (upstream).

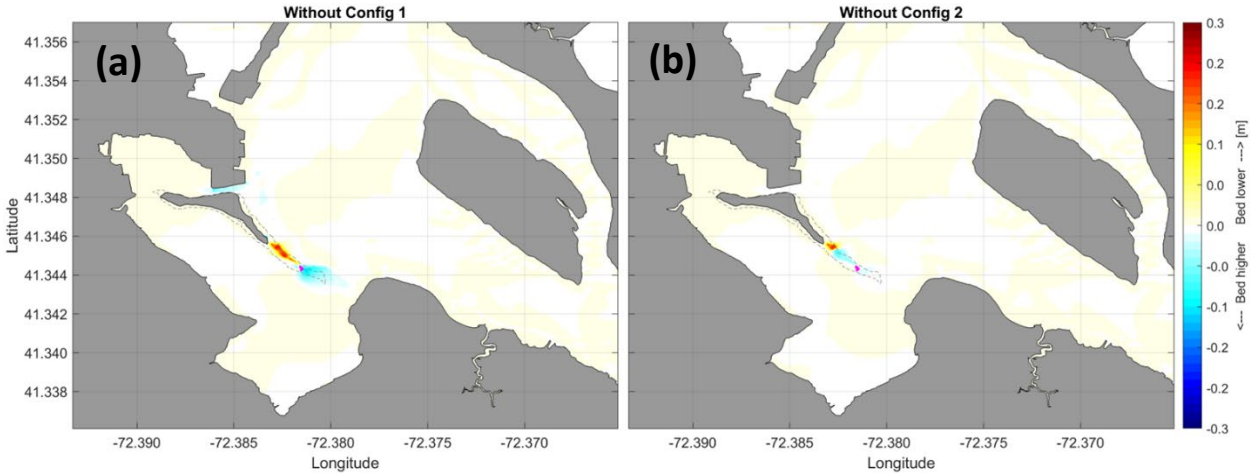

Figure S 5. Relative difference in bed level in the absence of Envirotube larger Configuration 1 (panel a) and smaller Configuration 2 (panel b) over the broader domain, including the river channel, for simulation Period P1. The historical outline of the Island (1991) from the DSAS is shown as a gray dashed line.

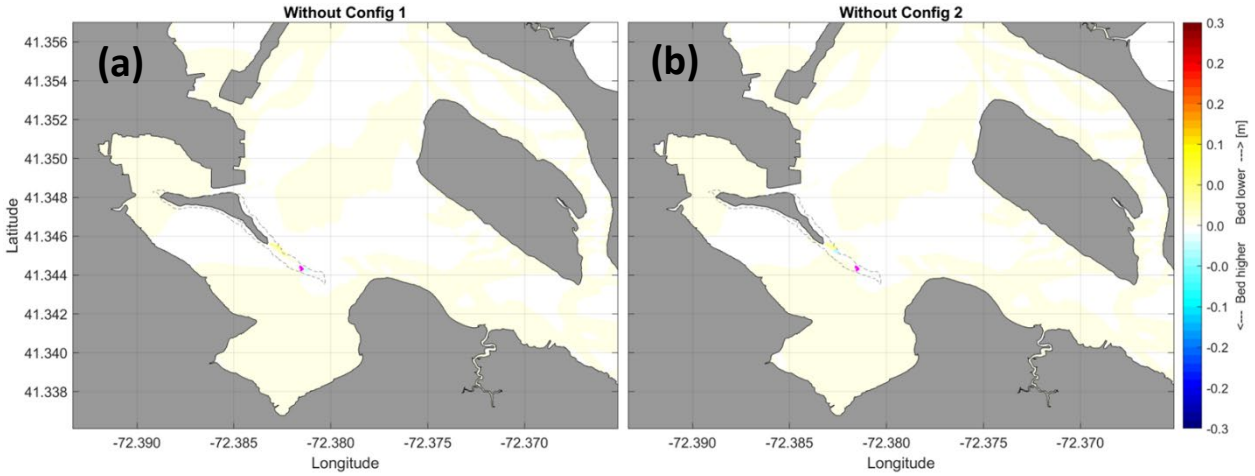

Figure S 6. Relative difference in bed level in the absence of Envirotube larger Configuration 1 (panel a) and smaller Configuration 2 (panel b) over the broader domain, including the river channel, for simulation Period P2. The historical outline of the Island (1991) from the DSAS is shown as a gray dashed line.

***